

SYNTHESIS, CHARACTERIZATION, AND CATALYTIC ACTIVITY  
OF NOVEL CU(II)-CALIX[6]ARENE COMPLEXES

THESIS

Presented to the Graduate Council  
of Texas State University-San Marcos  
in Partial Fulfillment  
of the Requirements

for the Degree

Master of SCIENCE

by

Derric Michael Borthwick, B.S.

San Marcos, Texas  
August 2006

## **DEDICATION**

This work is dedicated to all of my family and friends that have helped me get to where I am at today.

## ACKNOWLEDGEMENTS

I would like to thank Dr. Michael Blanda for offering me a great opportunity and letting me work in his lab; also Dr. Kevin Lewis and Dr. Wendi David for their support in my research. I would also like to thank Dr. Gary Beall for all of his time and effort as a mentor and professor. I feel my time at Texas State University-San Marcos has been invaluable, and hope my future success is a testament to the many great experiences I have endured here.

This manuscript was submitted on July 19<sup>th</sup>, 2006.

## TABLE OF CONTENTS

	Page
ACKNOWLEDGEMENTS.....	iv
LIST OF FIGURES.....	vii
LIST OF ILLUSTRATIONS.....	ix
CHAPTER	
I. INTRODUCTION.....	1
Thesis Proposal	
II. MOLECULAR DESIGN .....	11
Nomenclature and Conformations of Calix[6]arenes	
Synthetic Strategy	
Selectively Substituting the A and D Rings in the Lower Rim	
Preparing the Ligand	
Attaching the Ligand	
Copper Adducts	
III. RESULTS AND DISCUSSION OF COMPOUNDS 4 AND 5 .....	20
Structural Observations of 4	
Structural Observations of 5	
Modeling the Substitution Behavior with 4 and 5	
IV. RESULTS AND DISCUSSION OF COMPOUNDS 6 AND 7 .....	26
Structural Observations of 6	
Structural Observations of 7	
Copper Complexation in 7	

V. NUCLEIC ACID HYDROLYSIS STUDIES.....	40
Gel Electrophoresis Studies	
VI. MATERIALS AND METHODS.....	42
Materials	
Preparation of <b>1A</b>	
Preparation of <b>1B</b>	
Preparation of <b>2A</b>	
Preparation of <b>2B</b>	
Preparation of <b>3A</b>	
Preparation of <b>3B</b>	
Preparation of the Ligand	
Preparation of <b>4</b>	
Preparation of <b>5</b>	
Preparation of <b>6</b>	
Preparation of <b>7</b>	
UV-Vis experiments	
Mass Spectrometry Experiments	
Gel Electrophoresis Experiments	
Molecular Modeling Experiments	
REFERENCES.....	59
APPENDIX.....	63

## LIST OF FIGURES

<b>Figure 1.1</b> RNAi mechanism; from the Dharmacon RNAi interference guide, 2004.....	1
<b>Figure 1.2</b> Nuclease A active site; taken from J. Biol. Chem., Vol. 280, Issue 30, 27990-27997, July 29, 2005 .....	3
<b>Figure 1.3</b> TACI ligands .....	4
<b>Figure 1.4</b> ATCUN complexes from J. Am. Chem. Soc. 2005, 127, 8408-8415.....	5
<b>Figure 1.4</b> Oligonucleotide nuclease mimics from Nuc. Acids Res. 2003, 31, 1416-1425.....	6
<b>Figure 1.5</b> Calix[4] nuclease mimics.....	7
<b>Figure 1.6</b> Modeled dinuclear complex .....	9
<b>Figure 2.1</b> Calix[6]arene numbering system .....	11
<b>Figure 2.2</b> Modes of interconversion.....	12
<b>Figure 2.3</b> Designation of orientation, from Calixarenes Revisited; Gutsche, 1998 .....	13
<b>Figure 2.4</b> Synthesis diagram .....	15
<b>Figure 3.1</b> $^1\text{H}$ spectrum of <b>4</b> in $\text{CDCl}_3$ at $30^\circ\text{C}$ .....	20
<b>Figure 3.2</b> ESI-MS data for compound <b>4</b> .....	21
<b>Figure 3.3</b> Accelrys Cerius <sup>2</sup> minimized model of compound <b>5</b> .....	24
<b>Figure 4.1</b> $^1\text{H}$ spectrum of <b>6</b> in $\text{CDCl}_3$ at $50^\circ\text{C}$ .....	26

<b>Figure 4.2</b> $^{13}\text{C}$ DEPT spectrum of <b>6</b> .....	27
<b>Figure 4.3</b> $^1\text{H}$ NMR spectrum of <b>7</b> .....	28
<b>Figure 4.4</b> X-ray structure of <b>7</b> .....	29
<b>Figure 4.5</b> ESI-MS data for <b>7</b> with (1:1:1:1 – $\text{Mg}^{2+}:\text{Zn}^{2+}:\text{Ni}^{2+}:\text{Cu}^{2+}$ ) .....	30
<b>Figure 4.6</b> Mole ratio plot .....	31
<b>Figure 4.7</b> Hill plot.....	33
<b>Figure 4.8</b> ESI-MS data of <b>7</b> with and without amounts of copper. [From top to bottom: free host, host +0.5 eq].....	34
<b>Figure 4.8</b> 1:1 Cu-calix[6]arene ( <b>7</b> ) model.....	37
<b>Figure 4.9</b> Bond lengths in 1:1 complex.....	38
<b>Figure 4.10</b> 2:1 Cu-calixarene model and a close up of the second copper .....	39
<b>Figure 5.1</b> Gels <b>1</b> and <b>2</b> from left to right.....	40

## LIST OF ILLUSTRATIONS

<b>Illustration 1</b> Crystal Structure of 7 .....	64
<b>Illustration 2</b> Unit Cell of 7 .....	65

# CHAPTER I

## INTRODUCTION

The conserved, RNAi induced cleavage of targeted mRNA in biological systems proceeds from the complexation of an antisense oligonucleotide and the RNA induced silencing complex (RISC)<sup>1</sup>. The RISC complex then cleaves mRNA targets sharing homology with the bound 21-23 base RNAi strand (**Figure 1.1**)<sup>2</sup>.

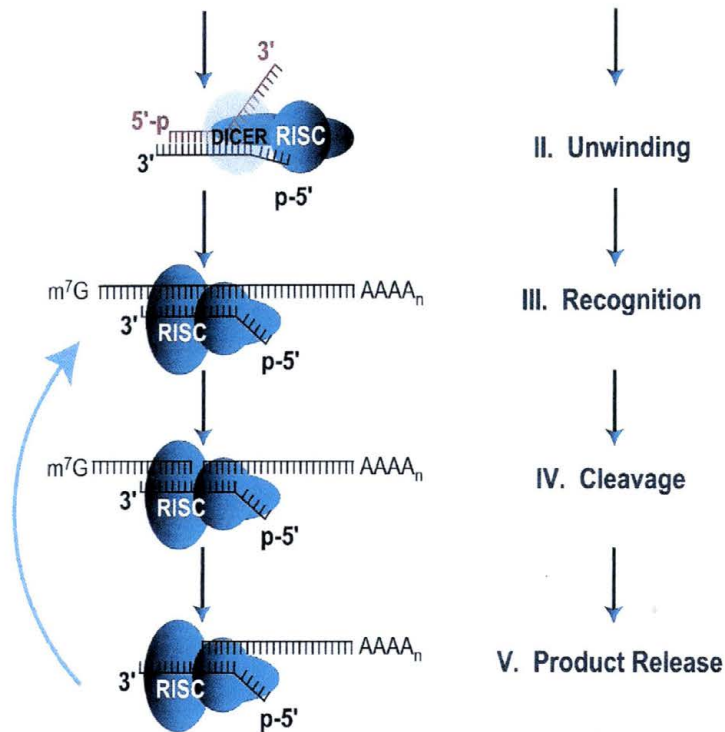


**Figure 1.1** RNAi mechanism; from the Dharmacon RNAi interference guide, 2004.

While the specific mechanism of the RISC system itself is not of particular concern to this research, the principal of site directed catalysis of nucleic acids (steps III, IV, and V in **Figure 1.1**) proves to be a meaningful inspiration; doing so would allow one to engineer synthetic nuclease mimics with many applications in basic research and medicinal therapies.

The RISC complex is an efficient and highly specific catalytic system capable of cleaving mRNA. The RISC pathway is also a very complex biological process, yet the idea of site directed catalysis itself is less convoluted. A common motif found in natural nuclease activity is the recurrent incidence of multiple heteroatoms; usually oxygen, nitrogen (frequently as a Schiff base), or both. The heteroatoms serve a two fold purpose in breaking the phosphodiester bond; after complexing metals, or acting as an acid or base, a concerted effort is made to stabilize transition states thereby facilitating catalysis<sup>3</sup>. Aspartate, histidine, and glutimate would be possible residues found in enzyme active sites capable of catalyzing nucleic acid cleavage as a result of metal complexation. For example, within the DRGH prosite-characterized family of divalent metal dependant, nonspecific nucleases, Nuclease A requires  $Mn^{2+}$  or  $Mg^{2+}$  to hydrolyze the phosphodiester bond with a histidine residue acting as the acid/base (**Figure 1.2**)<sup>4</sup>.

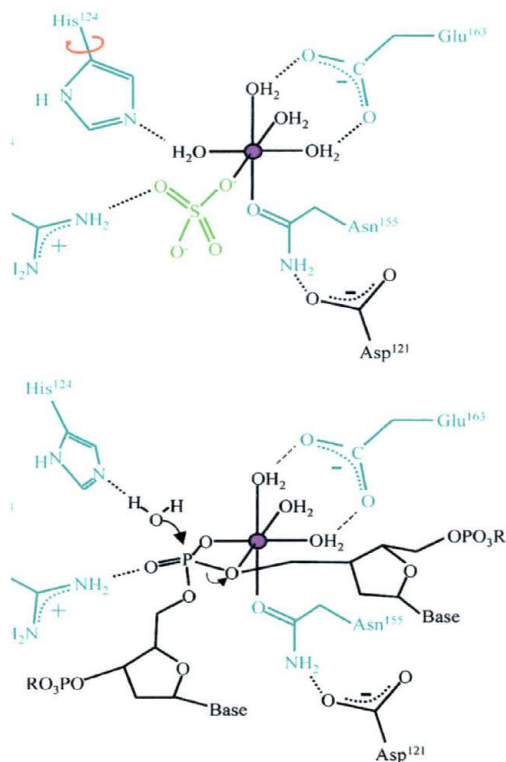
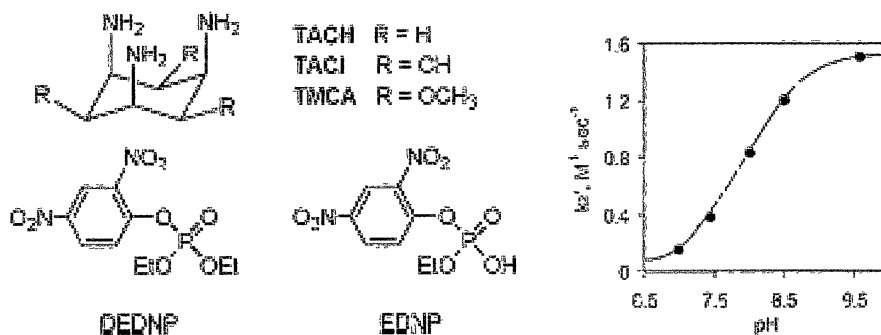


**Figure 1.2** Nuclease A active site; taken from *J. Biol. Chem.*, Vol. 280, Issue 30, 27990-27997, July 29, 2005.

For many nuclease mimics, the use of metal binding ligands is also a widely accepted technique for achieving phosphodiesterase activity with mono-, bi-, and tri-dentate moieties having nitrogen and/or oxygen present<sup>5-13</sup>. Metals typically chelated in these models are Cu(II) and Zn(II). This is because they are unlike their Co(III) and lanthanide(III) counterparts that are either toxic, or form unwanted byproducts<sup>14</sup>. Some of the structurally simplest biomimics developed by Tonellato *et. al.*, are the Cu(II)-TACI complexes, derived from, *all-cis*-2,4,6,-

triamino-1,3,5-trihydroxycyclohexanes<sup>15</sup>. The TACI complexes from Tonellato *et. al.* show efficient catalytic hydrolysis achieved from their mononuclear Cu(II) complexes.



Inorganic Chemistry, Vol 44 No. 7, 2005 2313

Figure 1.3 TACI ligands.

In addition, the optimal first order rate happens to coincide with the pK<sub>a</sub> of water; a tell-tale sign for a hydrolytic mechanism. It is also worth noting that the active site of NucleaseA happens to be optimally tailored for complexation of a hydrated metal ion<sup>16,17</sup>. The resulting hydroxyl group that is formed will act as the nucleophile initiating the hydrolysis reaction. Accordingly, it is of no surprise to see a pH dependence correlating to these slightly basic conditions for the presence of hydroxyl groups in synthetic models as well.

Other systems modeled from biological inspirations are the ATCUN complexes<sup>18</sup>, and also Cu(II) complexes embodied within an oligonucleotide<sup>19</sup>. Work done on the ATCUN (amino terminal Cu<sup>2+</sup> and Ni<sup>2+</sup> binding) models from Yin and Cowan produced a small molecule that is comprised of the amino acid sequence GGH (glycine, glycine, histadine). Normally, the active site of a given enzyme will be a three dimensional pocket where the participating residues will not be found in sequence. The folding patterns of the enzyme will actually place the residues within proximity of one another. The ATCUN model is actually a naturally occurring peptide motif that can be found in certain albumins.<sup>20</sup> Accordingly, it has been demonstrated that this motif has a high affinity for Cu(II)<sup>21</sup> and Ni(II)<sup>22</sup>. The sequential occurrence of this motif also makes it a realistic synthetic target. The resulting ATCUN-Cu(II) complex resulted in the conversion of super coiled DNA, to nicked open circle and linear dsDNA at a rate of  $\sim 39 \text{ M}^{-1} \text{ s}^{-1}$ .

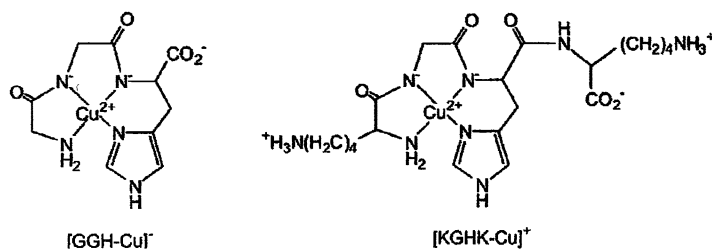


**Figure 1.4** ATCUN complexes from J. Am. Chem. Soc. 2005, 127, 8408-8415.

For the Cu(II) complexes that contains an oligonucleotide, Inoue *et al.* integrated copper binding ligands within an oligonucleotide to achieve site directed catalysis, which is also the goal of this research. The success of Inoue's work was limited. Site specific cleavage was achieved, but at a high cost in kinetic rate activity. Typical first order rate constants were around  $0.38 \text{ h}^{-1}$ . The free rotation of the copper complex within the ssRNA prevented any success with earlier models. As a result of this, Inoue used rigid linkers (PL<sub>n</sub>) for connecting the chelating ligands and the nucleotide (see **Figure 1.4**).

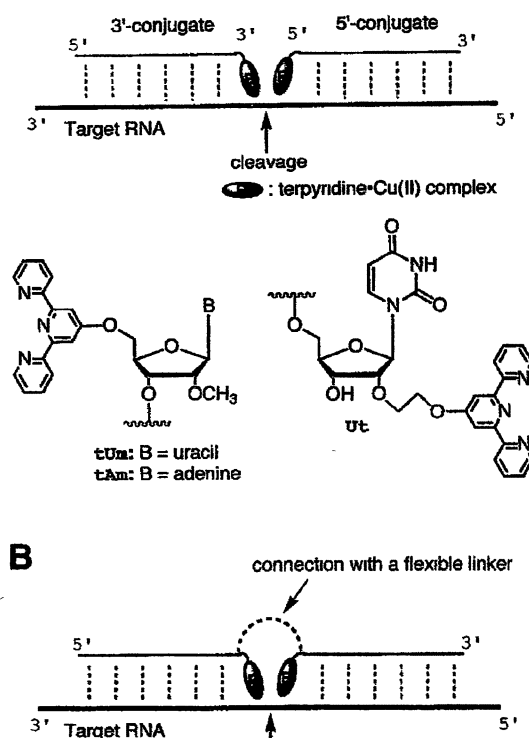


**Figure 1.4** Oligonucleotide nuclease mimics from *Nuc. Acids Res.* 2003, 31,

1416-1425.

The need for a rigid linker dramatically lowered the kinetic rate constants even though there was success in the goal of site directed catalysis. A more flexible candidate that mimics the behavior of that of an actual enzyme is more desirable. This is what led us to a calixarene-based nuclease mimic. Calixarenes are known for their flexibility and work from Reinhoudt has already seen success with di-nuclear Cu(II)-calix[4]arenes<sup>3</sup>.

*Catalytic Phosphate Diester Cleavage*

*J. Am Chem Soc., Vol 120, No. 27, 1998 6727*

Chart 1

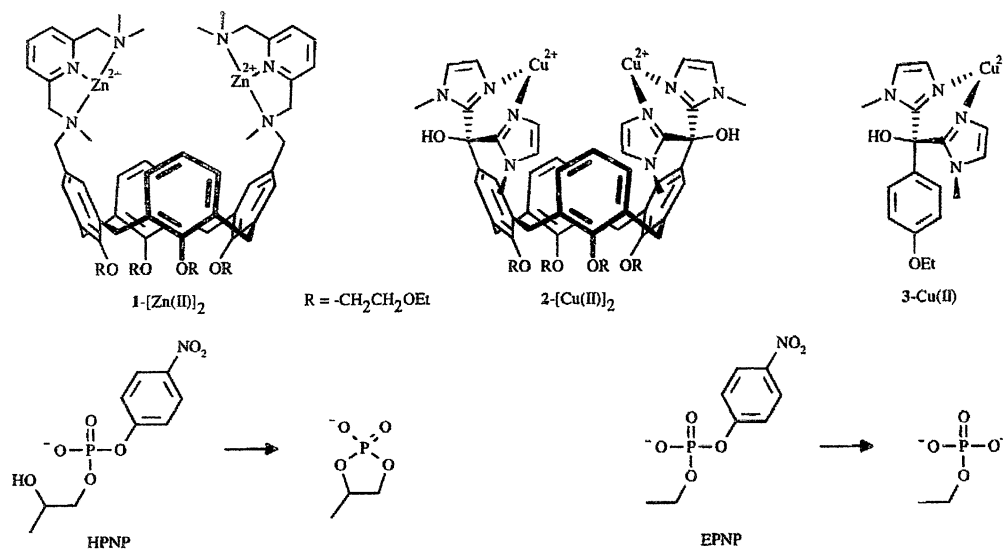


**Figure 1.5** Calix[4] nuclease mimics.

These imidazole containing di-nuclear complexes hydrolyze the synthetic nuclease substrate HPNP (see **Figure 1.5**) at a rate of  $\sim 30 \times 10^5 \text{ M}^{-1} \text{ s}^{-1}$ . This is proof

that the flexible calixarenes are capable of catalyzing non-specific phosphodiester bond hydrolysis at excellent rates. A similar behavior is also seen in pH dependence on the first order rate constant, which appears to be optimal at a slightly basic pH of 7.2.

### Thesis Proposal

Given the abundance of synthetically and naturally occurring imidazole moieties in phosphodiesterases, this study was focused on the construction of a tetra-imidazole functionalized calix[6]arene with the intent of complexing copper and facilitating nucleic acid hydrolysis. Due to the paramagnetic properties of Cu(II), complexation was primarily investigated through X-ray crystallography, UV-Vis spectroscopy, mass analysis, and corroborative computational models. However,  $^1\text{H}$  and  $^{13}\text{C}$  NMR were the primary means of characterization for the free host. The calixarene contains a high degree of symmetry and do not require complex NMR analysis methods, yet DEPT studies in addition to  $^{13}\text{C}$  will be employed in tandem to ensure proper chemical shift assignments by differentiating between methyl, methylene, and methylene carbons. Knowing the conformation of the free host was also necessary for determining the correct interpretation of results from copper complexation studies. Crystal data was also

used for input in molecular models using the Accelrys Cerius<sup>2</sup> software program to model the copper complexation in a theoretical environment for additional evidence. Crystal data input into the modeling program was also used for theoretical validation of modeled scenarios *in silico*. For example, first generation models showed a stable dinuclear complex, however, these models assumed a cone conformer where all of the oxygens are in the same plane in the lower rim.

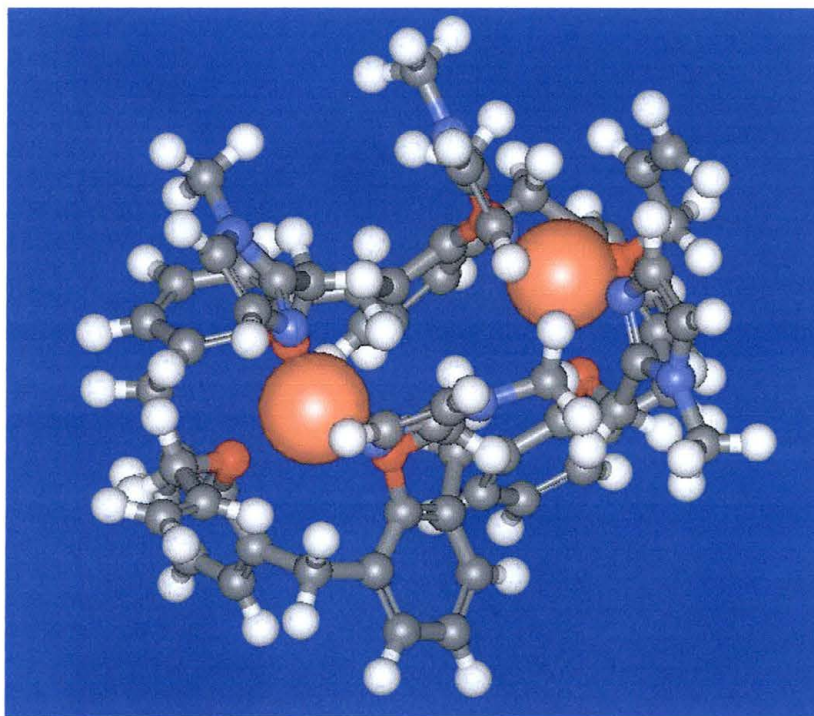


**Figure 1.6** Modeled dinuclear complex.

Other observable binding data were extracted from uv-vis spectra. The charge transfer band was determined by measuring the spectrum of the free host and observing the growth of a particular band upon the addition of copper. Two different methods of analysis was used to determine stoichiometric binding relationships between the calix[6] and Cu(II). Corroborative data from Hill plots and the mole ratio method allowed for an estimate of the most prevalent complexes, and it was determined that multiple species exist in solution concurrently.

In addition to the synthesis and characterization portions of this thesis, we used biochemical methods for the analysis of phosphodiester bond hydrolysis in double stranded oligonucleotides. Pre-cast acrylamide gels will be used for quantification of any cleavage taking place. Conditions were set at a slightly basic environment to help initiate the proposed hydrolytic mechanism. In addition to this, cleavage was also observed under other varying conditions such as copper/ calixarene ratios, while using free host (calixarene) and free guest (metal) for controls. The nucleic acids were visualized in the gels using an ethidium bromide staining solution, then washed, and exposed to UV light. The biological studies are intended to be preliminary in nature; there was no attempt to study rates or pH dependence in great depth at this stage.

## CHAPTER II

### MOLECULAR DESIGN

#### Nomenclature and Conformations of Calix[6]arenes

Shown below is the numbering system for calix[6]arene framework.

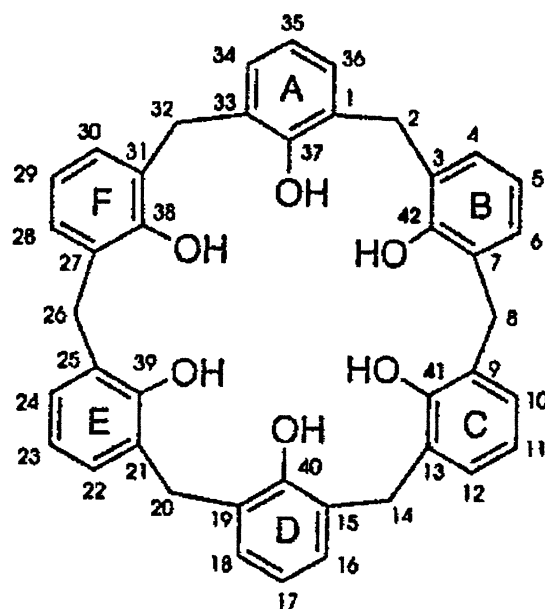


**Figure 2.1** Calix[6]arene numbering system.

According to this numbering scheme, the correct name for the structure is calix[6]arene-37,38,39,40,41,42 hexol. The calix[6]arenes have an upper rim and a

lower rim designated by positions 37, 38, 39, 40, 41, and 42 make up the lower rim. The positions 5, 11, 17, 23, 29, and 35 comprise the upper rim. The upper and lower rims are the primary areas for appending groups onto the calixarene framework. For ease of convention, the rings are commonly referenced in an alphabetical manner; A-F. Depending on the conformer, the alphabetical designation usually begins with A being assigned to a given reference ring.

Calix[6]arenes are conformationally mobile structures capable of ring interconversion. Ring interconversion can occur by two possible modes of motion. The ring can rotate through the annulus at the upper or lower rim. Substitutions at the upper and lower rim will also affect the ability to rotate by increasing the barrier of inversion. Modes of interconversion can be seen in

**Figure 2.2.**

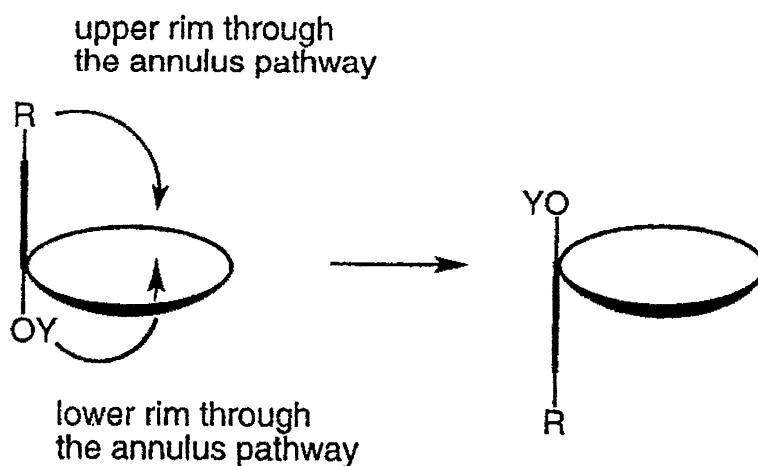


**Figure 2.2** Modes of interconversion.

Common names have been associated with these scenarios, such as the cone and alternate conformers. Relative orientation is designated as up (u) or down (d), as well as in (i) and out (o). The total combination of interconverted rings and orientation are summarized in **Figure 2.1**.

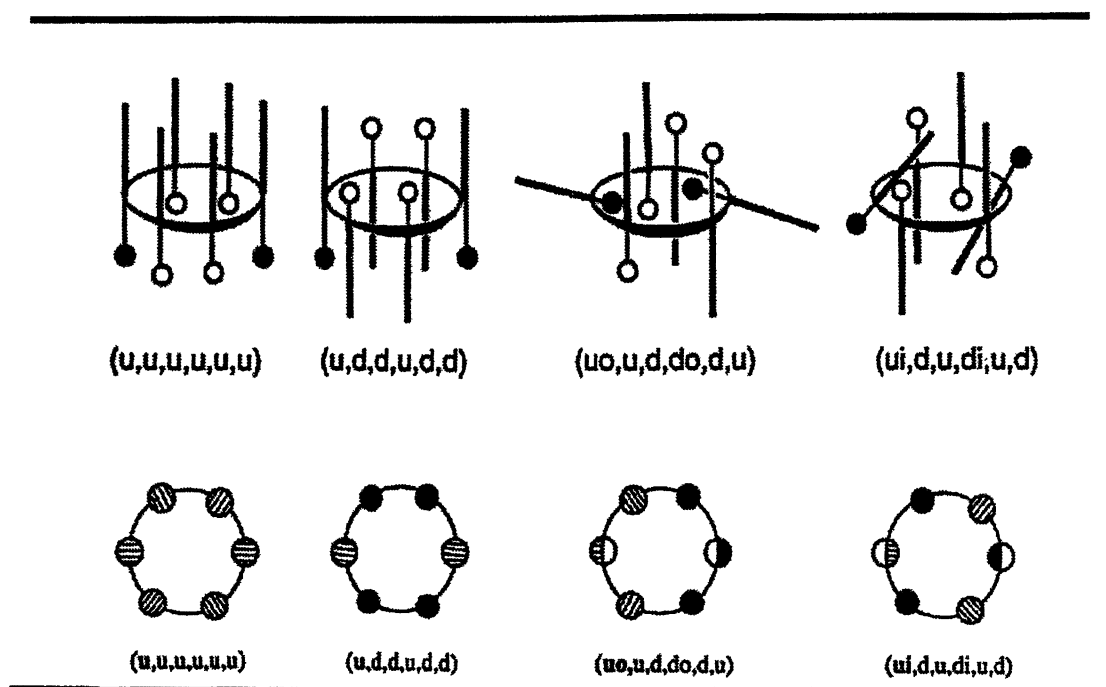


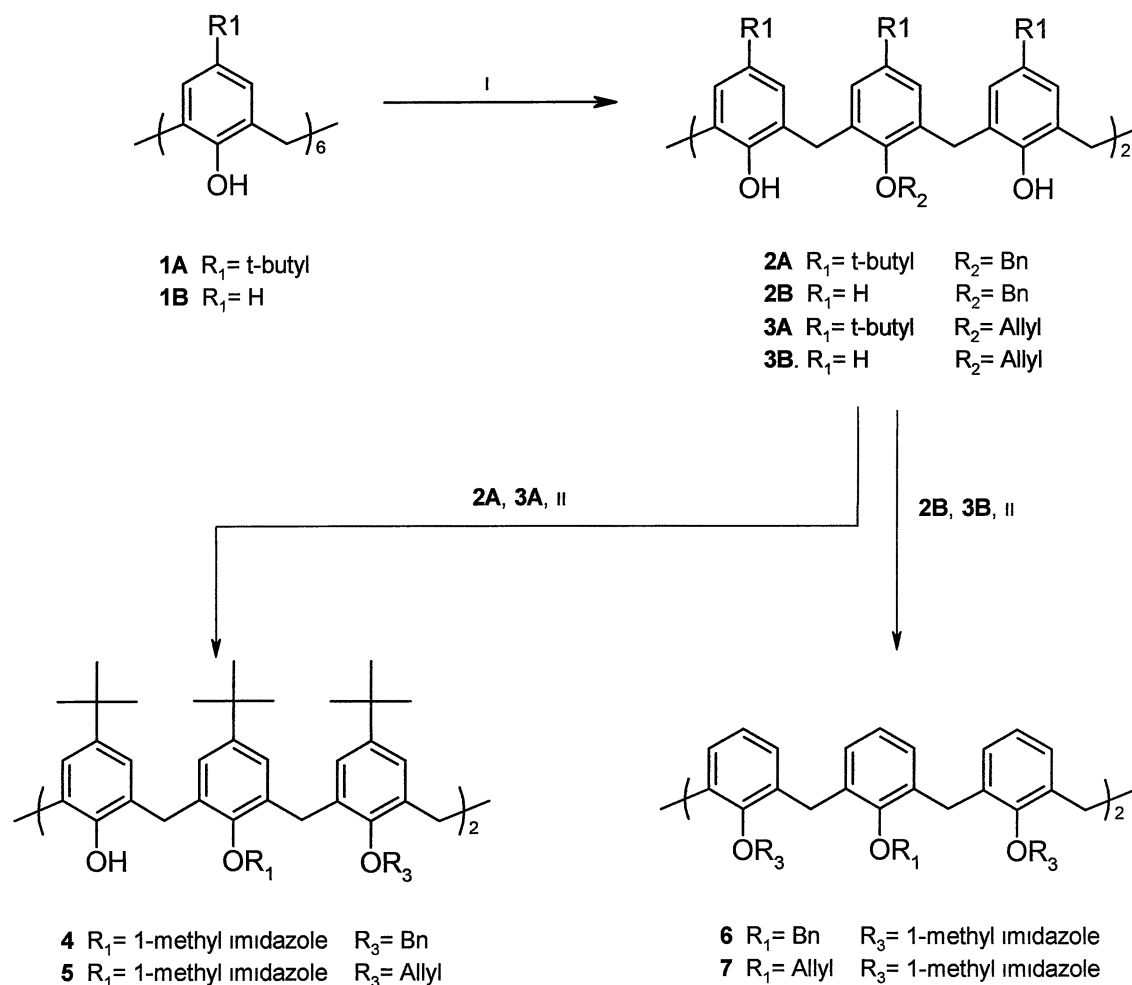
**Figure 2.3** Designation of orientation, from *Calixarenes Revisited*; Gutsche, 1998.

Due to the ring interconversion, two families of compounds were synthesized and studied to learn their effects on binding divalent metals with the appropriate ligands. The first family that was studied is referred to as the

alkylated series. The alkylated series has the upper rim positions substituted with large, bulky *t*-butyl groups. The dealkylated series has a proton in place of the *t*-butyl groups. The upper rim was the only variance between the two series of analogues.

### Synthetic Strategy

All of the calix[6]arene complexes and their precursors, including the 1-methyl imidazole ligand, were synthesized for this study. The two parent calixarenes (**1A** and **1B**) were synthesized as previously described<sup>23</sup>. Both the alkylated and dealkylated series of analogues were studied in a parallel manner to correlate structure-function relationships associated with the hexa-*tert*-butyl functionalization of the upper rim, as in compound **1A**, for both synthetic approach and the effects of structural mobility.



I = 7eq. (CH<sub>3</sub>)<sub>3</sub>SiOK, 3eq. Bn-Br or Allyl-Br, 9:1 THF/DMF, 18-20 hrs under N<sub>2</sub>; II = 30eq. NaH, 10eq. 2-chloromethyl -1-methyl imidazole, 9:1 THF/ DMF, 45 min. under N<sub>2</sub>.

**Figure 2.4** Synthesis diagram.

### Selectively Substituting the A and D Rings in the Lower Rim

To achieve a tetra-functionalized biomimic, the A and D rings were initially substituted with two different blocking. Either benzyl or allyl groups were appended in anticipation of later removal, coupling of the site directing

groups, or additional binding of the divalent guest. Benzylic residues have been specifically chosen for efficient protection and deprotection of the A and D rings for placing the site directing groups after the four remaining rings are substituted with the imidazole ligands. For the allyl groups, molecular models also show cooperative binding of the Cu(II) guest, further stabilizing the copper complex (**Figure 1.6**).

Selectively functionalizing the A and D rings was easily accomplished by utilizing the sterically hindered base, potassium trimethyl silanolate, to deprotonate the slightly acidic phenolic residues in the lower rim. Only the A and D rings were deprotonated, eventually resulting in the nucleophilic attack of the benzylic or allylic electrophile (usually as a halogenated analogue; allyl bromide or bromo-methyl benzene). This efficient reaction typically afforded the diether compounds **2&3** in 96% yield. The various reaction conditions and electrophiles employed can also be seen in **Figure 2.4**.

### Preparing the Ligand

Due to the nature of this work, a histidine-like ligand (1-methyl imidazole) was chosen to construct the metal binding site. Substituting 2 or 4 of the remaining phenolic residues with the imidazole moieties provided final host

compounds. The imidazole ligand was been chosen because of its structural similarities with histidine. Even in the synthetic nuclease mimics, we see a high selectivity for copper, ultimately resulting in hydrolytic phosphodiesterase activity. Furthermore, a tetra-functionalized cone conformer would allow for a dinuclear Cu(II) complex, where the B, C, E, and F rings would carry the imidazole moieties in the lower rim.

An overnight pressure vessel reaction with formaldehyde and 1-methyl imidazole yields 1-methyl-2-hydroxymethyl imidazole. The hydroxyl group is then converted to a halogen (chlorine) to serve as a better leaving group.

In all, the ligand was prepared in less than 24 hours with relatively good yield. However, special attention was given to the chlorination step. Any trace amounts of contaminants spoil the reaction due to the high reactivity of the thionyl chloride. These contaminants, in particular, include other alcohols and/or carbonyl containing compounds. To minimize possible contamination, the starting material was usually rinsed twice with ether and dried before the addition of the thionyl chloride.

### Attaching the Ligand

For our parallel studies, both alkylated and de-alkylated analogues were substituted with the imidazole ligand. A THF/DMF solvent mixture was utilized, and the calixarenes were allowed to mix briefly with an excess of base, NaH. Reaction conditions in the literature suggested refluxing over a couple of hours. However, conditions were optimized to yield a minimum amount of byproducts, whereby the length of the reaction time was shortened and kept slightly cool, around room temperature. Reaction conditions were optimized to yield product that was able to be cleaned without the use of column chromatography. A two-step crystallization process was employed to bring the product to high purity. Attempting to chromatograph the imidazole functionalized calixarenes on a silica column resulted in a poor recovery due to the extremely high retention on silica.

### Copper Adducts

The proposed biomimic is comprised of a calixarene molecule with bound copper to facilitate hydrolysis of the phosphodiester bond. The copper adducts were formed by dissolving the calixarene in a dichloromethane/methanol mix to permit solvent compatibility with copper (II) salts; primarily

Cu(II) NO<sub>2</sub>. The copper salts were then added to the solution in the desired stoichiometric ratios and studied using UV-Vis spectroscopy.

## CHAPTER III

### RESULTS AND DISCUSSION OF COMPOUNDS 4 AND 5

#### Structural Observations of 4

A simple  $^1\text{H}$  NMR spectrum of **4** shows little resolution for complete structure elucidation. However, the  $^1\text{H}$  spectrum does suggest three distinctly different  $^1\text{H}$  environments in the typical t-butyl region (0.2-1.8ppm), which correlates with a di-substituted calixarene (di-imidazole-di-hydroxy-di-benzyl) and a fluxional structure with multiple conformers.

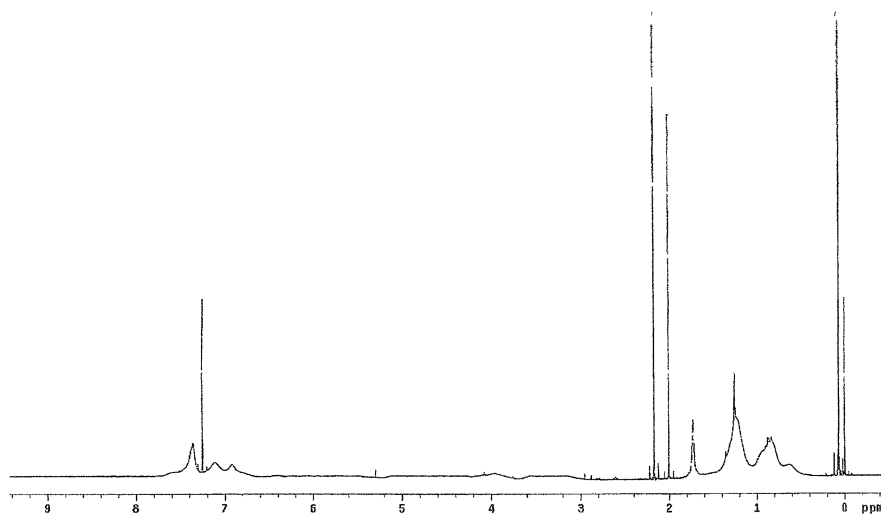


**Figure 3.1**  $^1\text{H}$  spectrum of **4** in  $\text{CDCl}_3$  at  $30^\circ\text{C}$ .

In other words, there are three different *t-butyl* environments represented by the ring systems carrying the benzyl groups, imidazole groups, and the unsubstituted rings (hydroxyl groups) in the lower rim. A di-substituted calixarene was neither expected nor intended for this study; however, it was intended to compare the alkylated and de-alkylated series to reveal any behavior such as this. ESI-MS analysis further supports the hypothesis of a di-substituted calixarene as well. The desired  $M^+$  ion was expected around 1530 m/z (molecular weight of 1529). The ESI-MS spectrum of **4** reveals an m/z of high intensity ( $5 \times 10^8$ ) at 1342, i.e. 1530 m/z minus 187.

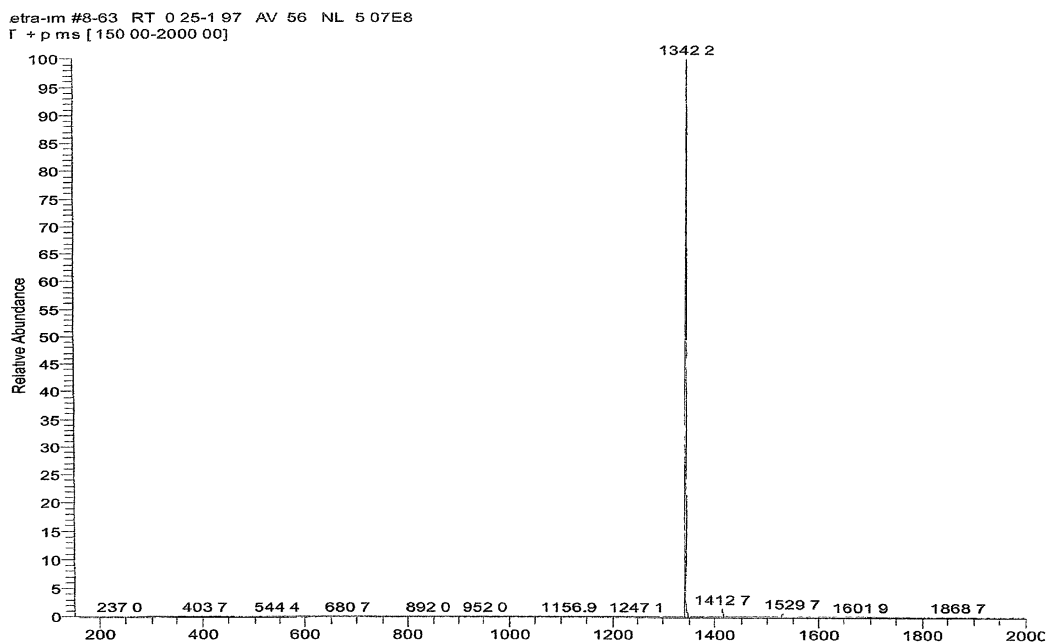


**Figure 3.2** ESI-MS data for compound **4**.

Replacing two of the four expected imidazole moieties in the lower rim with hydrogens results in a net mass difference of 188 (-95-95+2), confirming the functionalization of only two of the four remaining rings in the lower rim. A crystal structure has yet to be obtained, and will be necessary for further conformational analysis and determination of inherent chirality. Of the four remaining positions to be substituted in the lower rim, the B-C-E-F rings, there are six possible arrangements for the two imidazole moieties to occupy the lower rim. The six arrangements are actually comprised of two pairs of constitutional isomers and one pair of enantiomers. The two imidazole moieties can be adjacent (B-C, or E-F positions), orthogonal (B-E or C-F positions), or distal to one another (B-F or C-E positions). For the reaction mechanism, the first imidazole has equal probability of substituting any of the four positions. The position the first imidazole takes will sterically hinder the distal and adjacent positions for the subsequent imidazole substitution. The orthogonal position is thermodynamically most favorable, hence the assumption of an inherently chiral calixarene. Furthermore, a distal or adjacent substitution pattern would result in more than three different *t-butyl* groups because of the resulting asymmetrical calixarene basket conformation.

## Structural Observations of **5**

Similar di-substitution behavior was observed when substituting the A and D rings with smaller functional groups. In compound **5**, allyl groups were used in place of benzyl groups, and the attempt to functionalize the remaining four rings in the lower rim resulted in the  $^1\text{H}$  spectrum showing three distinctly different *t-butyl* chemical shifts as well. The substitution behavior appears to be the same in regards to the regioselectivity on the lower rim. Observing another di-substituted calixarene shows that smaller groups on the A and D rings do not impede with, or relieve, any steric interferences when substituting with the imidazole moieties. Again, a di-functionalized calixarene was not the intended compound for metal complexation and phosphodiester bond hydrolysis.

## Modeling the Substitution Behavior with **4** and **5**

A di-substituted calixarene was constructed *in-silico* and the most stable conformers were examined using open forcefield calculations (also see experimental). Molecular models suggest inherently chiral **5**, and **4**, assume a pinched cone conformation with the C and F rings forming the ends of the

pinched cone in a quasi planar orientation. The designation of this orientation would be (uo, ui, ui, uo, ui, ui).

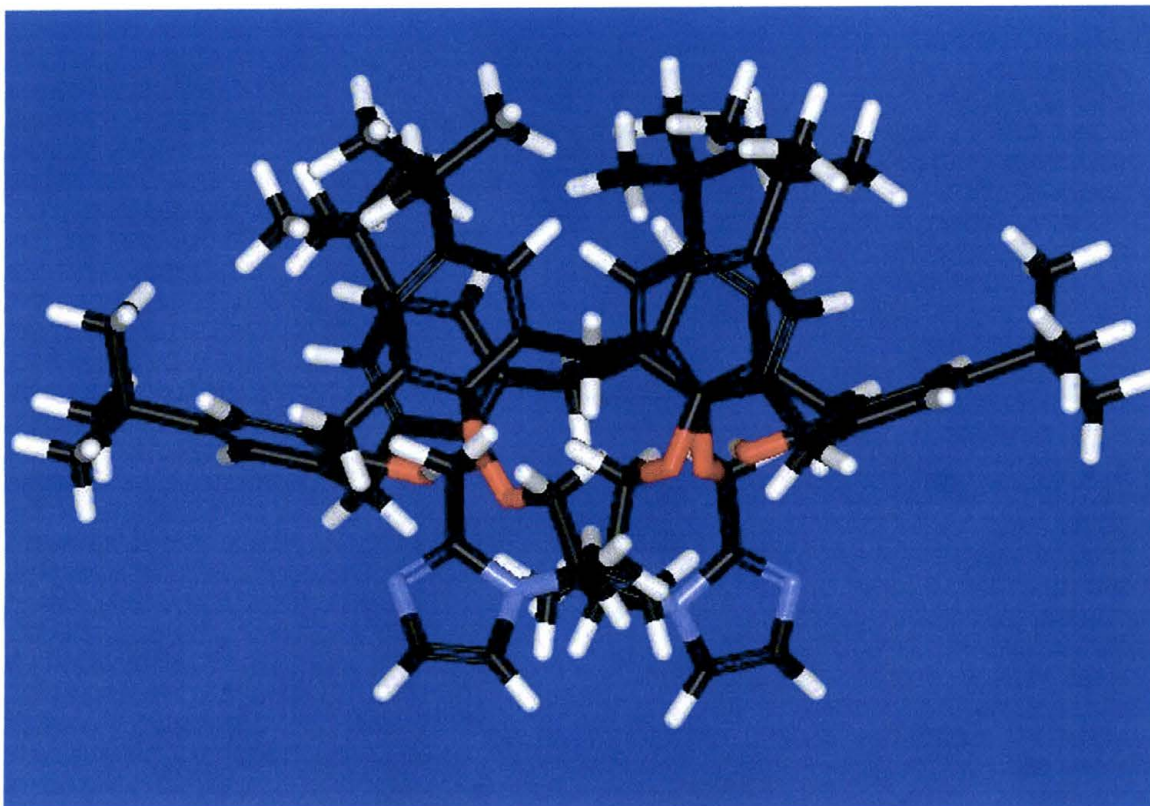


**Figure 3.3** Accelrys Cerius<sup>2</sup> minimized model of compound 5.

With the t-butyl groups on the upper rim, it is still possible for both upper and lower rim to rotate through the annulus, yet the upper rim inversion barrier increases when the lower rim is functionalized<sup>24,25</sup>. The molecular models further lead us to believe the stable pinched-cone conformation of the di-substituted

calixarene prevents further substitution of the C and F rings, by limiting accessibility through steric hinderance.

## CHAPTER IV

### RESULTS AND DISCUSSION OF COMPOUNDS 6 AND 7

#### Structural Observations of 6

The initial  $^1\text{H}$  spectrum obtained at room temperature reveals a conformationally mobile structure approaching its coalescence point in the NMR time scale. Heating 6 to  $50^\circ\text{C}$  is enough to equilibrate all of the calixarene conformations.

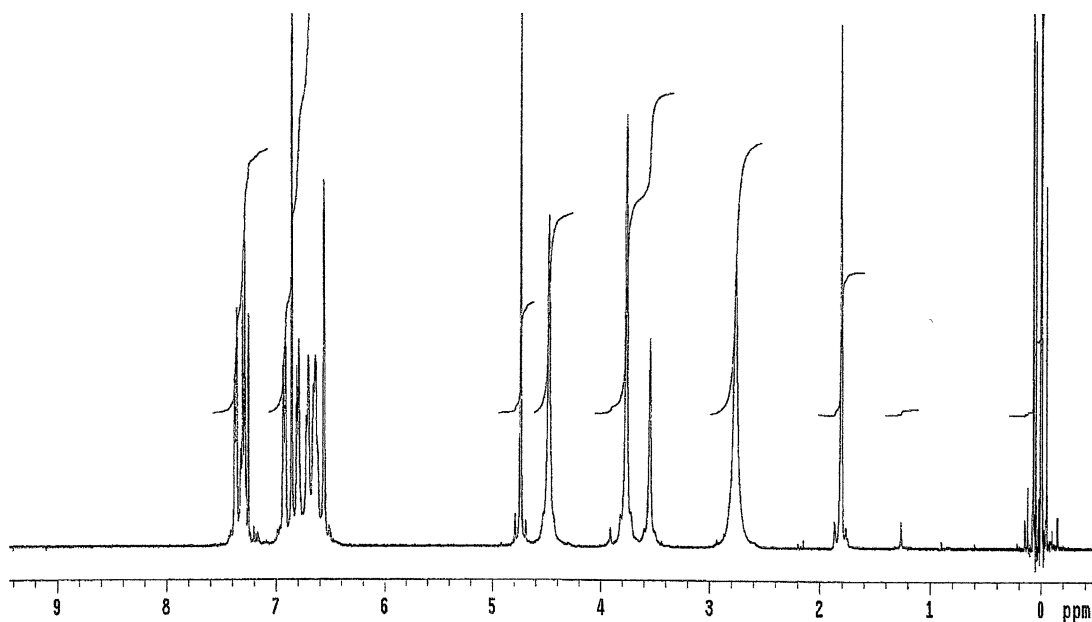


**Figure 4.1**  $^1\text{H}$  spectrum of 6 in  $\text{CDCl}_3$  at  $50^\circ\text{C}$ .

Most importantly we observed the CH<sub>3</sub> protons of the imidazole moieties at 2.78 ppm (s, 12H). The remaining CH<sub>2</sub> ether linkages and ArCH<sub>2</sub>Ar chemical shifts are found as a series of singlets between 3.58 and 4.76 ppm. The singlets in 2:1 ratios for both types of protons suggests a high degree of symmetry, however, they do not explicitly distinguish between the cone or 1, 2, 3, alternate conformers. The DEPT spectrum shows two types of bridging carbons at 31 ppm (31.25 ppm and 31.35 ppm at 2:1 intensity), suggesting both carbons are between *syn* oriented rings<sup>26</sup>, yet the <sup>1</sup>H NMR spectrum does not show a single conformer, making this rule inapplicable.

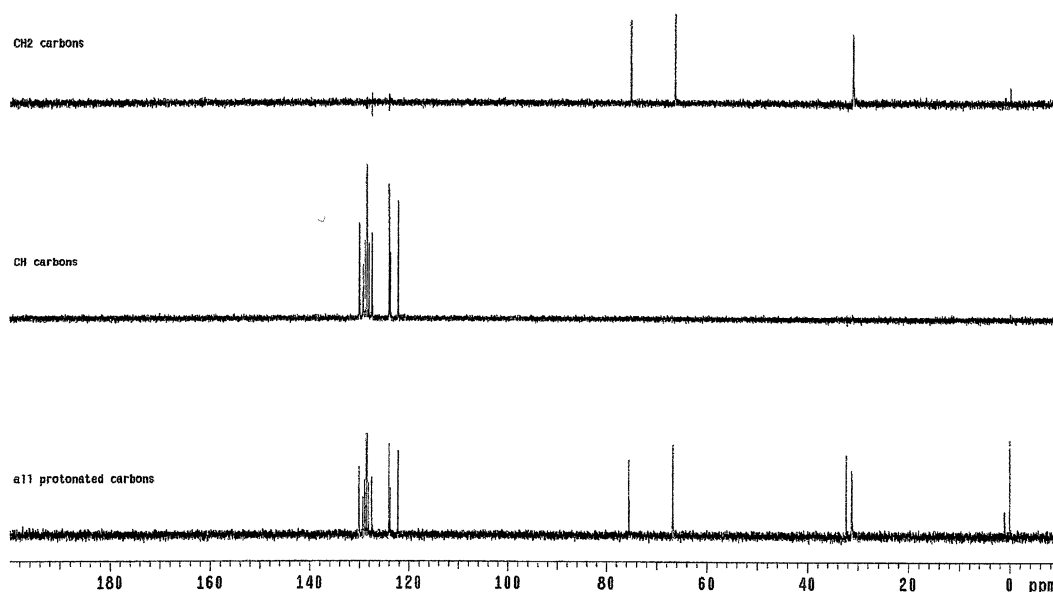
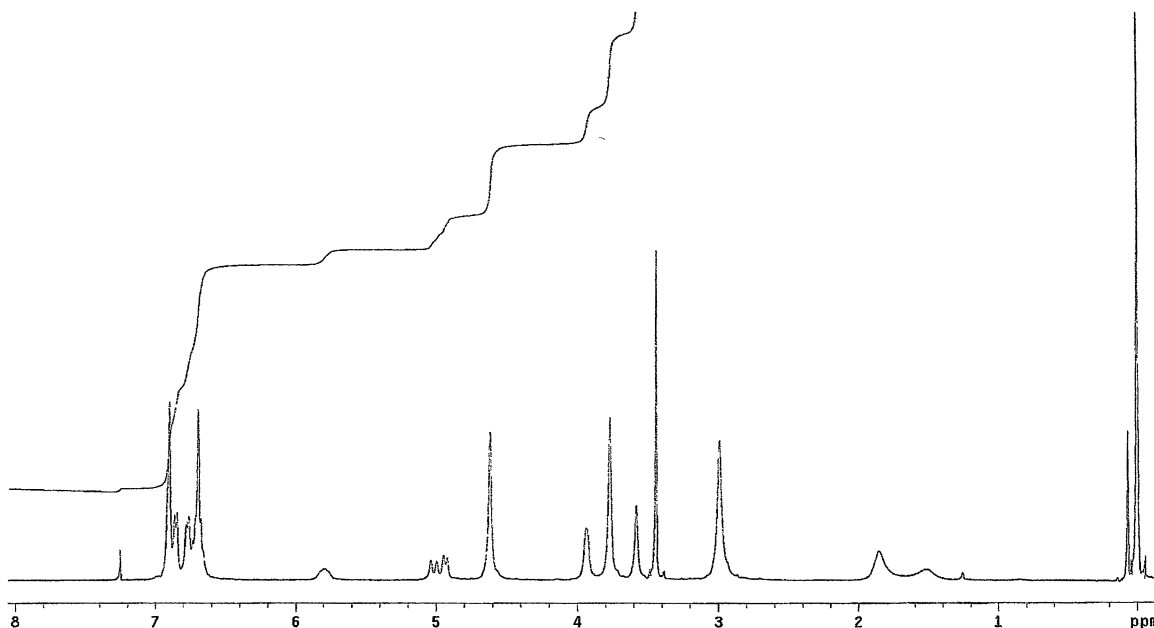


Figure 4.2 <sup>13</sup>C DEPT spectrum of 6.

The DEPT spectrum of **6** also confirms the CH<sub>3</sub> groups of the imidazole moieties at 32.5 ppm.

### Structural Observations of **7**

<sup>1</sup>H NMR data for **7** show similar behavior to **6**, as expected. It was necessary to heat the sample to 50°C in order to speed up the rotations about the ArCH<sub>2</sub>AR bonds and achieve sharper lines in the spectrum.



**Figure 4.3** <sup>1</sup>H NMR spectrum of **7**.

Along with the CH<sub>3</sub> groups at 3.01ppm (s, 12H), the allyl groups were observed as a doublet of doublets at 4.98ppm (4H, CH<sub>2</sub>'s of allyls) and a multiplet at 5.80ppm (2H, C-H of allyls). The terminal CH<sub>2</sub> carbons of the allyls show up in

the aromatic region at 123.7 and 123.9ppm in the  $^{13}\text{C}$  spectrum; data not shown.

The DEPT analysis also shows the desired substitution has been achieved.

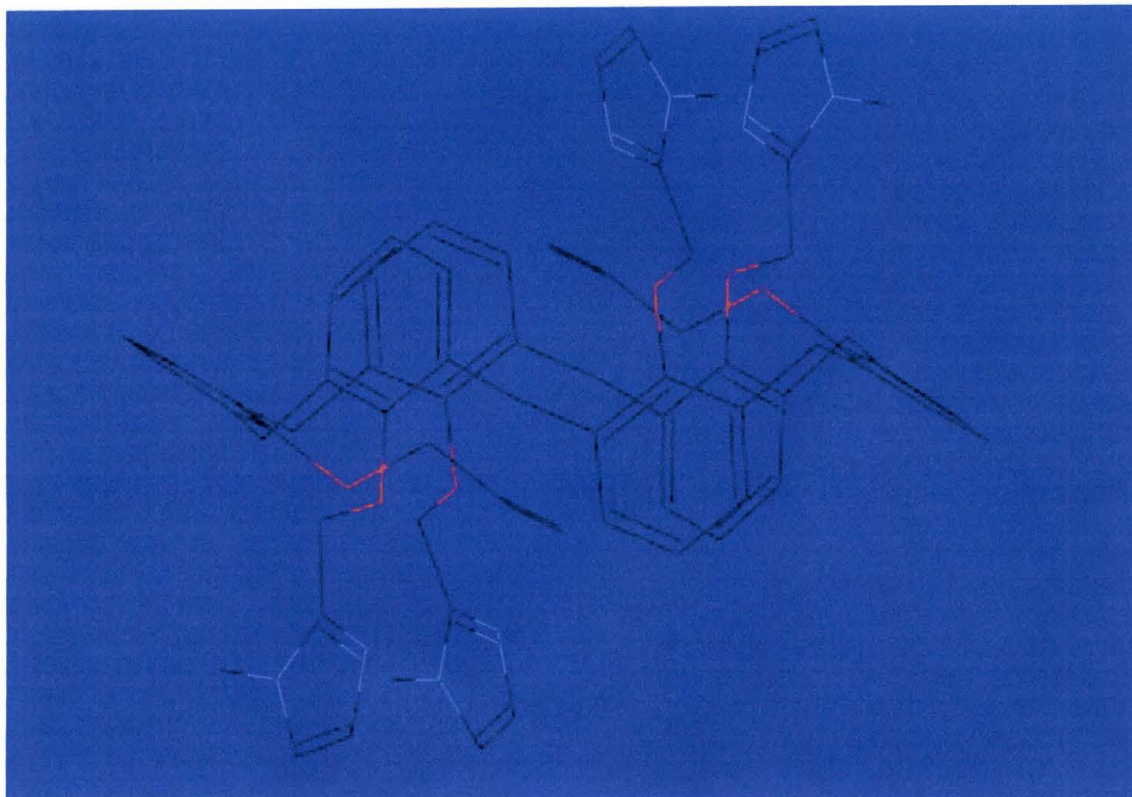


**Figure 4.4** X-ray structure of 7.

As seen in the crystal structure, the representative orientation for 7 is (uo, ui, ui, di, do, di). The resultant di-nuclear complex formed from the alternate conformer will have distances between copper centers greater than  $5\text{\AA}$ . Typical distances between di-nuclear Cu centers in other phosphodiesterase models ranges from 3- $5\text{\AA}$ . Copper complexation will be discussed in greater detail in the following section(s).

## Copper Complexation in 7

### *Binding Selectivity by Mass Spectrometry*

Initial ESI-MS studies were done in the lab of Dr. Brodbelt (UT Austin). The purpose of the study was to investigate the binding and/or binding selectivity of a handful of divalent metal guests. Of the metal guests ( $\text{Cu}^{2+}$ ,  $\text{Mg}^{2+}$ ,  $\text{Zn}^{2+}$ , and  $\text{Ni}^{2+}$ ), 7 exhibited a high selectivity for  $\text{Cu}^{2+}$ . The high selectivity is also accompanied with a low binding constant. The selectivity is not attributed to the ionic radius due to the similarities in size of the observed metals. When equal aliquots of all metal hosts were mixed in the gas phase with 7, the only species that were formed were 1:1 and 2:1 guest-host copper complexes. With a single equivalent of each metal added, approximately 23% free host was still present, with the remainder being 55%  $[\text{L}+\text{Cu}(\text{I})]^+$  (Cu(I) is seen due to the reduction under the ionization conditions), 17%  $[\text{L}+\text{Cu}(\text{II})]^{2+}$ , and 5%  $[\text{L}+2\text{Cu}(\text{I})]^{2+}$ .

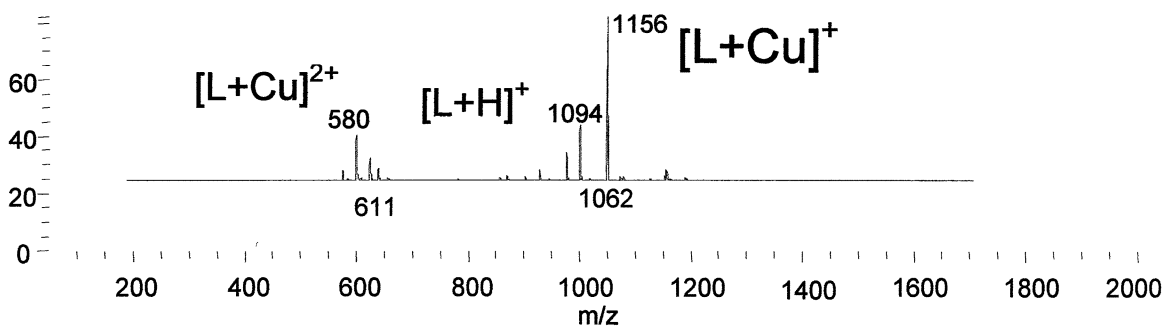


**Figure 4.5** ESI-MS data for 7 with (1:1:1:1 –  $\text{Mg}^{2+}:\text{Zn}^{2+}:\text{Ni}^{2+}:\text{Cu}^{2+}$ ).

*UV-Vis spectrometry studies*

Copper binding in the solution phase was confirmed by obtaining a uv-vis spectrum of the host **7** in the presence of  $\text{Cu(II)NO}_2$ . A charge transfer band was observed at 436 nm upon the addition of copper. This band was then referenced for quantifying the formation of the copper complexes in both of the mole ratio and Hill plot experiments. For the first method, the mole ratio of copper to free host was varied from 0-1 so the total number of moles of host and guest remain constant. Then the absorbance at 436 nm was monitored for a maximum within this range. Accordingly, the maximum absorbance reading for this range will directly correlate to the dominant species formed; i.e., 1:1 equals a mole fraction of 0.5, 2:1 is equal to a mole fraction of 0.67, and so on.

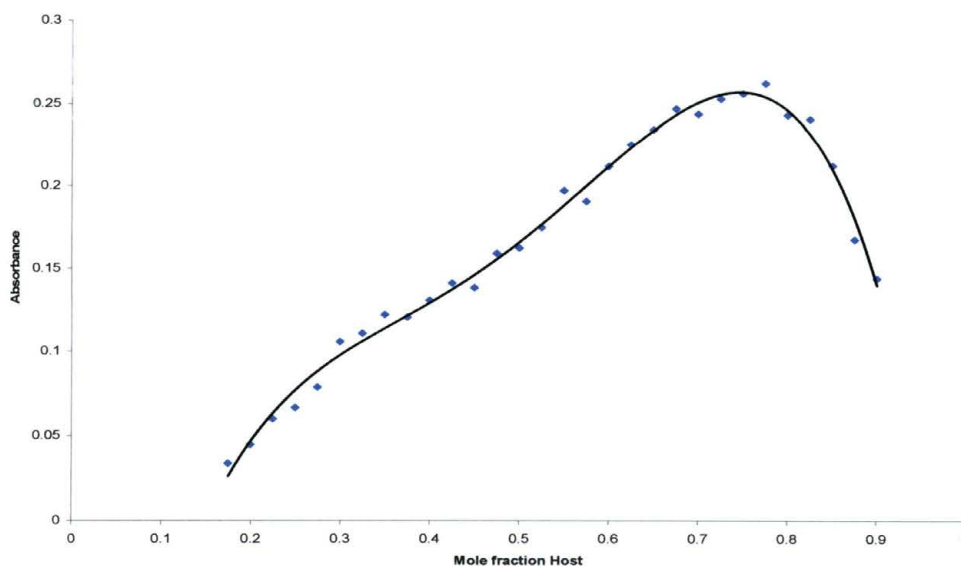


**Figure 4.6** Mole ratio plot.

The result from the mole ratio plot implicitly suggests the dominant species is approximately a 3:1 host-guest complex; however, it is highly unlikely that three hosts will form a complex with a single copper atom. As seen in the ESI-MS studies, there is still an incidence of free host, even in the presence of one full equivalent of guest. This would imply that a higher number of equivalents of host would be required to bind all of the copper, hence the 3:1 complex maxima. This is also supported by broadness in the peak that results from a relatively lower binding constant.

For the next experiment, the amount of calixarene was kept constant and copper was added until an increase in absorbance was no longer observed. When the absorbance no longer increases, it is assumed that the host has been saturated with guest. Therefore, the point at which the slope of the line becomes zero is equal to the equivalence of guest found in the dominant species.

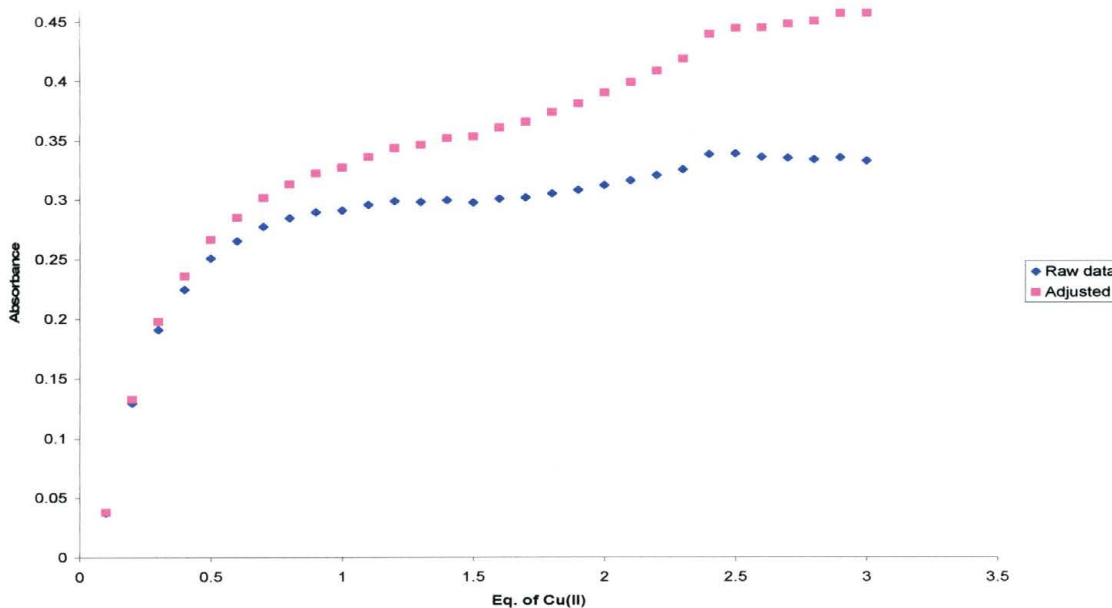


**Figure 4.7** Hill plot.

The Hill plot further reveals the complexity of the copper binding in 7. The plot is characterized by a broad slope change and approaches zero momentarily around 1.2 equivalents, but never completely levels out. This behavior demonstrates that 1:1 and some 2:1 complex is forming with a low binding constant, and the 2:1 complex becomes the more dominant species as the copper equivalence reaches a threshold as seen from the abrupt increase in slope at 2.5 equivalents. Additionally, there is never incidence of one single species in solution; i.e., only free host, 1:1, or 2:1 etc. This is extrapolated from the fact that the slope of the line never remains zero.



At 0.5 equivalents of copper, only ~22% of **7** has formed a complex, leaving 78% free host. The pattern is the same for 1:1 and 2:1, where roughly half of the copper is bound by the host. This pattern also decreases with increasing copper concentration. The host (**7**) will not become saturated until in the presence of approximately four equivalents of copper. Here we observe the most abundant peak at 1154 m/z, with no free host, and ~24% of the 2:1 Cu<sup>+1</sup>-calixarene complex present. The 2:1 complex does not become the dominant species in solution until after five equivalents of copper have been added. Even at 50 equivalents of copper, the 2:1 complex comprises only 33% of the species present (100 relative abundance; see appendix for additional spectra). This would explain why the mole ratio method suggests a dominant species being a 1:3 copper-calixarene complex since more copper is required to increase the absorbance significantly, and, from the Hill plot we see that the slope of the absorbance will not approach zero within the observed range since the calixarene has not yet been saturated.

### Modeling Copper Complexation

Further investigation *in silico* suggests copper complexation where the oxygen in the ether linkages, the Schiff base nitrogen in the imidazole moieties,

and the  $\pi$  system in the allyl groups all participate in binding copper. The first scenario that was modeled in the Accelrys Cerius<sup>2</sup> environment was a 1:1 host guest stoichiometry. The symmetry of the molecule allows the application of equal binding preference to the ABF or CDE portions of the calixarene (imidazole – allyl – imidazole) for 1:1 binding. Binding a single Cu<sup>2+</sup> atom lowered the overall energy of the molecule by 20 Kcal/mol. Binding two Cu<sup>2+</sup> atoms lowered the energy another 50Kcal/mol. This does not directly correlate with the uv-vis and mass spectrometric data that suggest the second copper bound has an even lower binding constant than the first. However, this does demonstrate that there is a re-organization energy barrier that is overcome by mass action to bind the second copper.

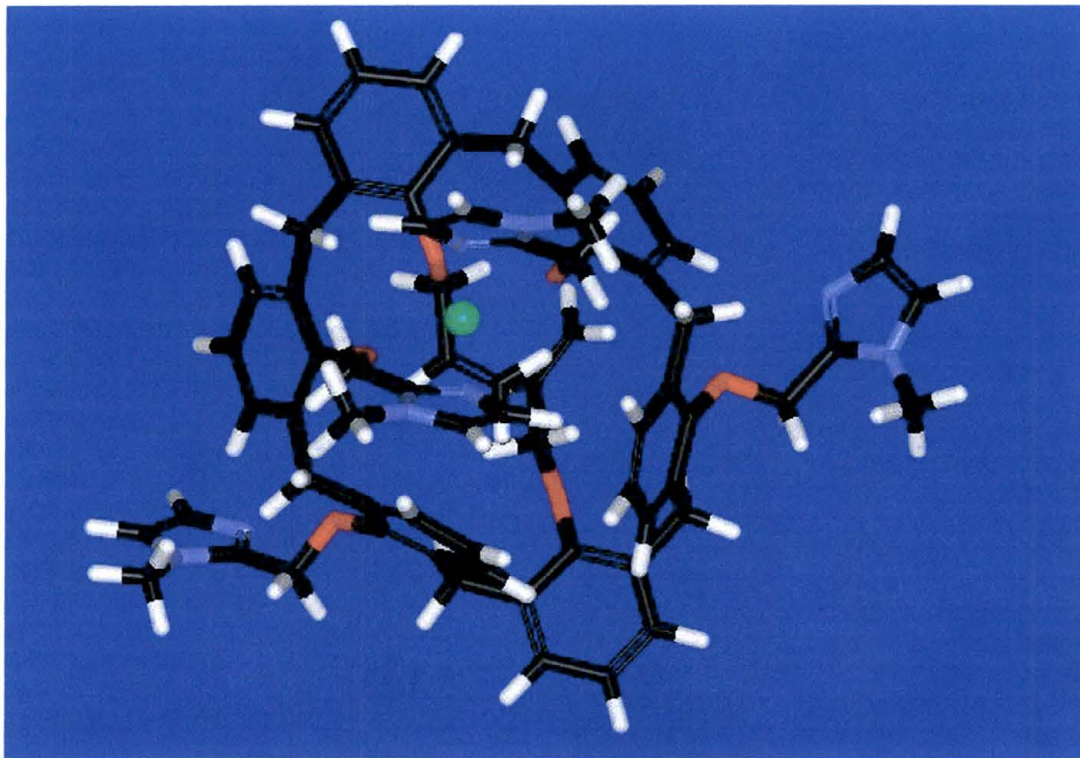


**Figure 4.8** 1:1 Cu-calix[6]arene (7) model.

Binding the first copper strains the calixarene basket and swings out the two remaining imidazoles as a result; seen in Figure 4.8. This is made possible by the hexa-coordinate binding geometry of the first bound copper.

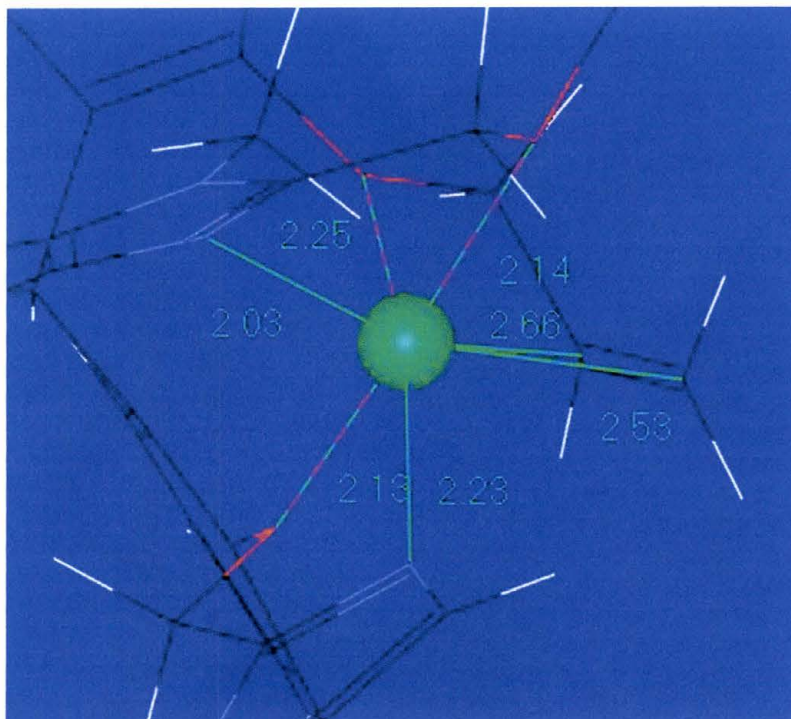


**Figure 4.9** Bond lengths in 1:1 complex.

Figure 4.9 shows the first copper bound to two of the nitrogens in the imidazoles, three oxygens in the ether linkages, and the pi system of one of the allyl groups. Bond distances are shown for both of the carbons in the allyl group to demonstrate that the  $\pi$  system is indeed centered on the copper atom. Same as the second copper, the initial copper was bound after overcoming the reorganization barrier due to the strain put on the basket of the calixarenehost.

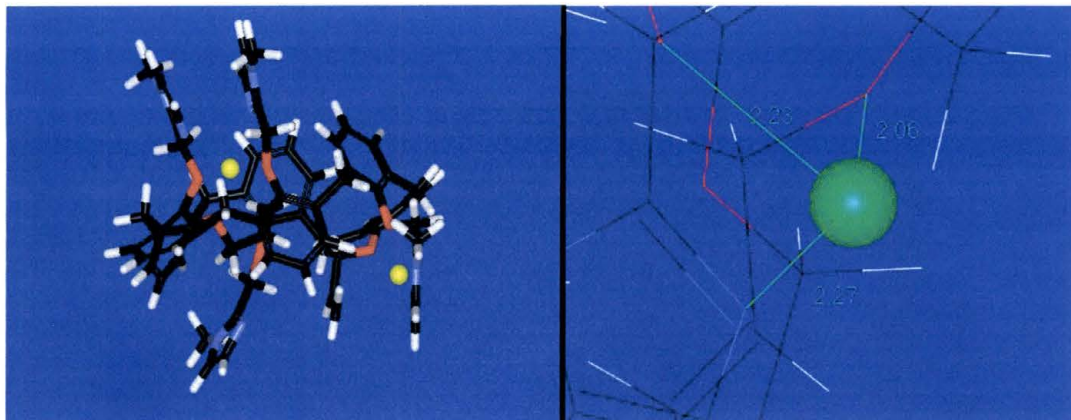


**Figure 4.10** 2:1 Cu-calixarene model and a close up of the second copper.

For the second copper to bind, the stress on the basket would distort the hexa-coordinate geometry or environment of the first copper, but still retain its overall integrity while the single imidazole swings in and binds the second copper along with two of the oxygens in the remaining ether linkages. Both of the re-organization barriers would explain the low binding constants while stabilizing, or lowering, the overall energy of the complex. However, this arrangement will prevent the first copper from becoming accessible to any nucleic acids and the second copper may not be capable of hydrolysis, being bound to a single imidazole and having a trigonal binding geometry.

## CHAPTER V

### NUCLEIC ACID HYDROLYSIS STUDIES

#### Gel Electrophoresis Studies

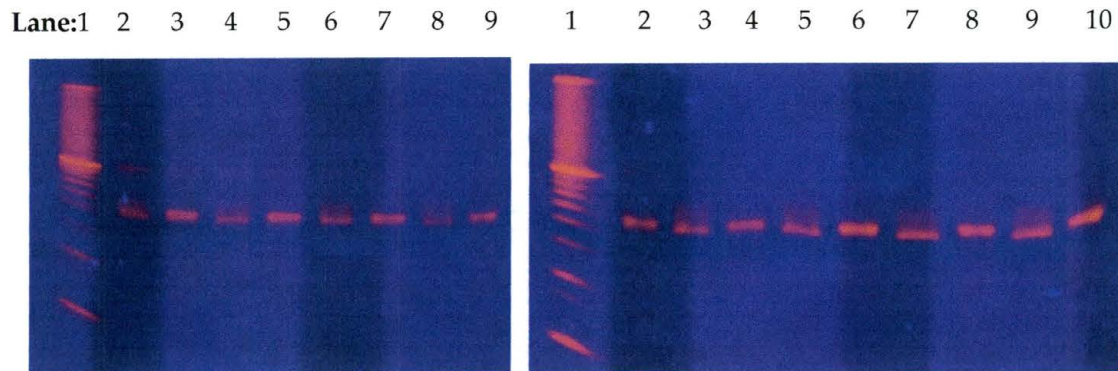


**Figure 5.1** Gels 1 and 2 from left to right.

Preliminary gel electrophoresis data suggest 7 does not show any hydrolytic activity within the experimental conditions employed; no nucleic acid models have been demonstrated to function in the environment of our experimental conditions. Two fragments of dsDNA of 50 bp each (poly AT and poly GC) were used for this experiment. It was intended to investigate any cleavage specificity between AT or GC base pairs. The lanes were assigned as such: Gel 1 - ln1 (10bp ladder), ln2 (AT only), ln3 (GC only), ln4 (AT +1eqCu), ln5 (GC +1eq Cu), ln6 (AT +1eq calix), ln7 (GC +1eq calix), ln8 (AT +1eq Cu +1eq

calix), ln9 (GC +1eq Cu +1eq calix); Gel2 – ln1 (10bp ladder), ln2 (GC +2eq Cu), ln3 (AT+2eq Cu +1eq calix), ln4 (GC +2eq Cu +1eq calix), ln5 (AT +4eqCu + 1eq calix), ln6 (GC +4eq Cu +1eq calix),ln7 (AT +4eq Cu +1eq calix),ln8(GC +6eq Cu), ln9 (AT +6eq Cu +1eq calix), ln10 (GC +6eq Cu +1eq calix). Considering the unexpected 1, 2, 3, alternate conformer and the complex copper binding stoichiometry may give insight to not having observed DNA cleavage. The first copper bound by 7 is bound in an octahedral coordination sphere and would not be likely to interact with any external species. The second copper bound has greater accessibility, yet it is bound to a single imidazole and two oxygens in the ether linkages. This arrangement has not been observed in any nucleic acid cleaving models. It must also be taken into consideration that the expected hydrolytic mechanism for this model is highly pH dependant, and this experiment only addressed one pH of 7.5. Both of the copper centers would also need to be brought into closer proximity to one another and this can be achieved by inducing a cone conformer with bulky groups in the upper rim.

## CHAPTER VI

### MATERIALS AND METHODS

See appendix for additional NMR spectra.

#### Materials

All reagents were purchased through Sigma-Aldrich and used as is unless otherwise specified. Both  $^1\text{H}$  and  $^{13}\text{C}$  NMR spectra were collected on a 400MHz Varian NMR. Chemical shifts ( $\delta$ ) in NMR data were referenced in ppm, relative to the internal standards TMS (for organic solvents) and  $\text{D}_2\text{O}$  (for aqueous solvents). Mass spec data for selectivity experiments were obtained from collaborations with the lab of Dr. Brodbelt at the University of Texas at Austin. In-house mass spec data was obtained using the electrospray ionization method with an LCQ ESI mass spectrometer. TLC analysis was done on pre-coated IB2-F silica gel plates. All reactions were done under technical grade Argon, except for the synthesis of the chloromethyl imidazole ligand. UV-Vis experiments were done on a Perkin Elmer spectrometer. All reagents and pre-cast gels for the hydrolysis studies were purchased from Invitrogen and used as directed by Invitrogen.

Preparation of 1A (5, 11, 17, 23, 29, 35-hexa-*p*-tert-butyl-37, 38, 39, 40, 41, 42-hexahydroxycalix[6]arene)

To a three neck, 3L round bottom flask equipped with a mechanical overhead stirrer, and a Dean–Stark trap, 100g (.67 mol) of 4-*tert*-butylphenol and 40g (1.33 mol) of paraformaldehyde were suspended in 1.5L of xylene. The mixture was allowed to stir for several minutes before adding 26.65 mL (0.34 eq's or 0.2363 mol) of rubidium hydroxide in a 50% wt. aqueous solution, via a 100mL syringe. The Dean-Stark trap was then filled to the upper joint with xylene. Finally, the reaction was allowed to reflux under argon for 20h. The round bottom and connecting arm of the Dean-Stark trap were also wrapped with fiberglass wool to contain the heat. During the first hour, the reaction mixture is expected to rise to reflux temperature and take the appearance of a celar, tea-like mixture with all of the reactants dissolved. After the 20 hours, the glass wool and heat were removed from the round bottom. The reaction mixture was cooled before filtering through a Buchner funnel. The filter cake was dried and then dissolved in two liters of  $\text{CHCl}_3$  and washed three times with 2N HCl. Emulsions arising from the washes were allowed to settle for several hours, and overnight on occasion. Either way, the organic layer should be clear to ensure good separation. The  $\text{CHCl}_3$  containing the product was dried over magnesium

sulfate and filtered. The solvent was then reduced, *in vacuo*, to a few hundred milliliters and recrystallized from 1L of methanol. The precipitate was filtered and rinsed with a small amount of acetone. The resulting pure white powder weighed 82g (72% yield): mp. 380-381°C; Rf =.63 in CHCl<sub>3</sub>/Hexane (3:4); <sup>1</sup>H NMR (400MHz, CDCl<sub>3</sub>) δ = 10.2 (s, ArOH, 12H), 7.10(s, ArH, 12H), 3.88 (s, ArCH<sub>2</sub>Ar, 12H), 1.25 (s, C(CH<sub>3</sub>)<sub>3</sub>, 54H). <sup>13</sup>C NMR (400 MHz, CDCl<sub>3</sub>) δ = 147.2, 144.2, 126.9, 126.1, 34.0, 33.1, 31.4.

#### Preparation of **1B** (37, 38, 39, 40, 41, 42-hexahydroxy Calix[6]arene)

In a 3L round bottom flask, 1.5L of toluene was stirred before adding 70g (.072 mol) of **1A** and 60g (0.731 mol) of phenol. Next, 115g (0.862 mol) of AlCl<sub>3</sub> was added and all of the reactants quickly dissolved. The reaction was then allowed to react for 48h under an argon atmosphere at room temperature. After the allotted time, the reaction was quenched by adding 1L of 2N HCl. The organic layer was then separated and the toluene was removed under vacuum. The residue was then dissolved in 1.5L of chloroform and washed twice with 2N HCl. The organic layer was then dried over magnesium sulfate and filtered. Again, the solvent was removed and the product was precipitated in 1.5L of methanol. The resulting precipitate (**2**) was pure white and weighed 39.1g

(85%yield): mp. 417-418°C;  $^1\text{H}$  NMR (400 MHz,  $\text{CDCl}_3$ )  $\delta$  = 10.4(s, ArOH, 6H), 6.7-7.4(m, ArH, 16H), 4.0 (s, ArCH<sub>2</sub>Ar, 12H).

Preparation of **2A** (5, 11, 17, 23, 29, 35-hexa-*p*-tert-butyl-37, 40-Dibenzyloxy-38, 39, 41, 42-tetrahydroxycalix[6]arene)

In a 2L round bottom equipped with a magnetic stirrer, 35.9g (0.037 mol) of **1A** and 27.1g (0.211 mol) of potassium trimethyl-silanolate was added to a mixture of 1.2L of THF and 120mL of DMF (9/1). The reaction mixture was then cooled in a 0°C ice bath for 15 minutes. Once cooled, 10.95mL of allylbromide was slowly added via a 50mL syringe. The reaction mixture was then allowed to react at room temperature for three hours. After which, the reaction solvent was removed under water aspirated vacuum to remove the THF and a mechanical high vacuum pump to remove the remainder of the DMF solvent. The residue that remained was dissolved in  $\text{CHCl}_3$  and washed three times with 2N HCl. The organic layer was removed and dried over magnesium sulfate then filtered. The filtrate was concentrated to about 100mL and the product was precipitated by pouring the solution in 800mL of hexane. The pure white precipitate was filtered, dried, and weighed 39.0g (96% yield):  $^1\text{H}$  NMR (400 MHz,  $\text{CDCl}_3$ )  $\delta$  = 8.03 (s, -OH, 4H), 7.36-7.94 (m, 10H), 7.2-6.78 (m, ArH, 24H), 5.86 (m, -CH=, 2H), 4.39 (d, -

OCH<sub>2</sub>-, 4H, J=6Hz), 3.94 and 3.78 (two s, ArCH<sub>2</sub>Ar, 12H), 1.23 (s, C(CH<sub>3</sub>)<sub>3</sub>, 36H), 0.89 (s, C(CH<sub>3</sub>)<sub>3</sub>, 18H). <sup>13</sup>C NMR (400MHz, CDCl<sub>3</sub>) δ = 132.9, 131.5, 129.3, 128.7, 128.5, 127.5, 127.1, 124.3, 121.5, 121.3, 120.2, 117.9, 76.1, 36.3, 34.1, 31.6, 31.5.

#### Preparation of **2B** (37, 40-Diallyloxy-38, 39, 41, 42-tetrahydroxycalix[6]arene)

In a 2L round bottom equipped with a magnetic stirrer, 20.g (.031 mol) of **1B** and 27.1g (0.021 mol) of potassium trimethyl-silanolate was added to a mixture of 1.2L of THF and 120mL of DMF (9/1). The reaction mixture was then cooled in a 0°C ice bath for 15 minutes. Once cooled, 10.95mL of benzylbromide was slowly added via a 50mL syringe. The reaction mixture was then allowed to react at room temperature for three hours. After which, the reaction solvent was removed under water aspirated vacuum to remove the THF and a mechanical high vacuum pump to remove the remainder of the DMF solvent. The residue that remained was dissolved in CHCl<sub>3</sub> and washed three times with 2N HCl. The organic layer was removed and dried over magnesium sulfate then filtered. The filtrate was concentrated to about 100mL and the product was precipitated by pouring the solution in 800mL of hexane. The pure white precipitate was filtered, dried, and weighed 39.0g (96% yield): <sup>1</sup>H NMR (400 MHz, CDCl<sub>3</sub>) δ = 8.09 (s, -OH, 4H), 7.09-6.89 (m, ArH, 24H), 6.76 (t, ArH, 4H, J=6.0Hz), 4.46 (d, -OCH<sub>2</sub>-, 4H,

$J=6\text{Hz}$ ), 3.94 and 3.78 (two s,  $\text{ArCH}_2\text{Ar}$ , 12H), 1.23 (s,  $\text{C}(\text{CH}_3)_3$ , 36H), 0.89 (s,  $\text{C}(\text{CH}_3)_3$ , 18H).  $^{13}\text{C}$  NMR (400MHz,  $\text{CDCl}_3$ )  $\delta$  = 162.5, 152.4, 151.8, 133.2, 131.8, 129.1, 128.9, 128.7, 127.5, 127.1, 125.5, 122.9, 121.7, 120.2, 118.5, 75.9, 36.4, 34.2, 31.5, 31.4.

Preparation of **3A** (5, 11, 17, 23, 29, 35-hexa-*p*-tert-butyl-37, 40-Diallyloxy-38, 39, 41, 42-tetrahydroxycalix[6]arene)

In a 2L round bottom equipped with a magnetic stirrer, 35.9g (0.037 mol) of **1A** and 27.1g (0.021 mol) of potassium trimethyl-silanolate was added to a mixture of 1.2L of THF and 120mL of DMF (9/1). The reaction mixture was then cooled in a 0°C ice bath for 15 minutes. Once cooled, 7.75mL of allylbromide was slowly added via a 10mL syringe. The reaction mixture was then allowed to react at room temperature for three hours. After which, the reaction solvent was removed under water aspirated vacuum to remove the THF and a mechanical high vacuum pump to remove the remainder of the DMF solvent. The residue that remained was dissolved in  $\text{CHCl}_3$  and washed three times with 2N HCl. The organic layer was removed and dried over magnesium sulfate then filtered. The filtrate was concentrated to about 100mL and the product was precipitated by

pouring the solution in 800mL's of hexane. The pure white precipitate was filtered, dried, and weighed 39.0g (96% yield)

#### Preparation of **3B** (37, 40-Diallyloxy-38, 39, 41, 42-tetrahydroxycalix[6]arene)

In a 2L round bottom equipped with a magnetic stirrer, 20g (0.031 mol) of **1B** and 27.1g (0.021 mol) of potassium trimethyl-silanolate was added to a mixture of 1.2L of THF and 120mL of DMF (9/1). The reaction mixture was then cooled in a 0°C ice bath for 15 minutes. Once cooled, 7.75mL of allylbromide was slowly added via a 10mL syringe. The reaction mixture was then allowed to react at room temperature for three hours. After which, the reaction solvent was removed under water aspirated vacuum to remove the THF and a mechanical high vacuum pump to remove the remainder of the DMF solvent. The residue that remained was dissolved in  $\text{CHCl}_3$  and washed three times with 2N HCl. The organic layer was removed and dried over magnesium sulfate then filtered. The filtrate was concentrated to about 100mL and the product was precipitated by pouring the solution in 800mL of hexane. The pure white precipitate was filtered, dried, and weighed 21.8g (96% yield).

### Preparation of the Ligand (N-methyl-2-chloromethyl imidazole)

Into a 350mL pressure vessel, was placed 30g (0.036 mol) of 1-methylimidazole and 120mL (0.5 mol) of formaldehyde (37% wt.) solution. The pressure vessel was then submersed to the solvent level-line in a sand bath. The bath was adjusted to 130°C, and the temperature was carefully monitored to prevent it from exceeding 150°C. After 15-16 hours, the mixture was slowly cooled to room temperature. Once cool, 100mL of a 50:50 solution of ethanol and conc. HCl was slowly added to the reaction mixture. The mixture was stirred for five minutes. The ethanol and water were then removed under reduced pressure, resulting in a viscous, clear to yellow syrup. This syrup was dissolved again in ethanol and the solvent was removed for a second time. The resulting syrup was then dissolved in a small amount of absolute ethanol and stirred in an acetone/dry ice bath until the N-methyl-2-hydroxymethyl imidazole HCl salt precipitated (42g, 78% yield). This salt was then washed with ether and dried. The HCl salt was slowly dissolved in 19.5 mL of thionyl chloride on ice in a 100mL round bottom and then refluxed for one hour. The thionyl chloride was removed under reduced pressure and the resulting crystalline powder was washed with ether then acetone to yield 10.1g (93% yield) of N-methyl-2-

chloromethyl imidazole.  $^1\text{H}$  NMR (400MHz,  $\text{D}_2\text{O}$ )  $\delta$  = 7.38 (s, 1H), 7.36 (s, 1H), 4.88 (s, 2H), 3.80(s, 3H).

Preparation of **4** (5, 11, 17, 23, 29, 35-hexa-*p*-tert-butyl-37, 40-Dibenzyloxy-38, 41-di(1-methylimidazolyl)oxy-39, 42-dihydroxycalix[6]arene)

In a 100ml round bottom flask, 40mL's of THF and 20mL's of DMF (9:1) were placed on a magnetic stirrer and set to mix. Then, 2.0g (0.0017mol) of **2A** were added to the round bottom and put in a 0°C ice bath for five minutes. Once the mixture has cooled it is removed from the ice bath. Next, 2.1g (0.051 mol) of NaH (as a 60% oil dispersion) was washed twice with hexane and added in small portions to the reaction mixture and allowed to stir for an additional fifteen minutes. Finally, 2.2 g (0.0102 mol) of N-methyl-2-chloromethyl imidazole were added portion-wise to the reaction mixture and allowed to react for one hour at room temperature under argon. After an hour, the THF was removed under reduced pressure and the high vacuum was required to remove an amount of DMF to achieve a final volume that is approximately 1/3<sup>rd</sup> the original volume, and allowed to cool while stirring. To the stirring solution, 300mL of de-ionized water was added drop-wise. The resulting precipitate was filtered and re-suspended in a mixture of 150mL of de-ionized water and 150mL of acetone and

let stir for 15 minutes. The product was filtered and re-suspended in another solution of hot methanol, then allowed to cool slightly and 50mL of acetonitrile and de-ionized water were added. When the mixture reaches room temperature it was filtered again, resulting in 1.73g (75 % yield) of pure white powder after drying overnight in a dessicator.  $^1\text{H}$  NMR (400MHz,  $\text{CDCl}_3$ )  $\delta$  = 7.3-6.8 (m, Ar-H, 22H), 1.2-0.8 (three s,  $\text{C}(\text{CH}_3)_3$ , 54H).

Preparation of **5** (5, 11, 17, 23, 29, 35-hexa-*p*-tert-butyl-37, 40-Diallyloxy-38, 41-di(1-methylimidazolyl)oxy-39, 42-dihydroxycalix[6]arene)

In a 100ml round bottom flask, 40mL's of THF and 20mL's of DMF (9:1) were placed on a magnetic stirrer and set to mix. Then, 2.0g (0.0019mol) of **3A** were added to the round bottom and put in a 0°C ice bath for five minutes. Once the mixture has cooled it is removed from the ice bath. Next, 2.3g (0.057 mol) of NaH (as a 60% oil dispersion) was washed twice with hexane and added in small portions to the reaction mixture and allowed to stir for an additional fifteen minutes. Finally, 2.4 g (0.0114 mol) of N-methyl-2-chloromethyl imidazole were added portion-wise to the reaction mixture and allowed to react for one hour at room temperature under argon. After an hour, the THF was removed under reduced pressure and the high vacuum was required to remove an amount of

DMF to achieve a final volume that is approximately 1/3<sup>rd</sup> the original volume, and allowed to cool while stirring. To the stirring solution, 300mL of de-ionized water was added drop-wise. The resulting precipitate was filtered and re-suspended in a mixture of 150mL of de-ionized water and 150mL of acetone and let stir for 15 minutes. The product was filtered and re-suspended in another solution of hot methanol, then allowed to cool slightly and 50mL of acetonitrile and de-ionized water were added. When the mixture reaches room temperature it was filtered again, resulting in 1.77g (75 % yield) of pure white powder after drying overnight in a dessicator. <sup>1</sup>H NMR (400MHz, CDCl<sub>3</sub>) δ = 7.3-6.8 (m, Ar-H, 22H), 5.95 (m, -CH=, 2H), 5.40 (d, =CH<sub>2</sub>, 2H, J=20.0Hz), 5.08 (d, =CH<sub>2</sub>, 2H, J=12Hz), 4.46 (d, -OCH<sub>2</sub>-, 4H, J=6Hz), 3.94 and 3.78 (two s, ArCH<sub>2</sub>Ar, 12H), 1.2-0.8 (three s, C(CH<sub>3</sub>)<sub>3</sub>, 54H).

Preparation of **6** (37, 40-Dibenzyloxy-38, 39, 41, 42-tetra(1-methylimidazolyl)oxy-dihydroxycalix[6]arene)

In a 100ml round bottom flask, 40mL's of THF and 20mL's of DMF (9:1) were placed on a magnetic stirrer and set to mix. Then, 2.0g (0.0024mol) of **2B** were added to the round bottom and put in a 0°C ice bath for five minutes. Once the mixture has cooled it is removed from the ice bath. Next, 3.0g (0.072 mol) of

NaH (as a 60% oil dispersion) was washed twice with hexane and added in small portions to the reaction mixture and allowed to stir for an additional fifteen minutes. Finally, 3.1 g (0.014 mol) of N-methyl-2-chloromethyl imidazole were added portion-wise to the reaction mixture and allowed to react for one hour at room temperature under argon. After an hour, the THF was removed under reduced pressure and the high vacuum was required to remove an amount of DMF to achieve a final volume that is approximately 1/3<sup>rd</sup> the original volume, and allowed to cool while stirring. To the stirring solution, 300mL of de-ionized water was added drop-wise. The resulting precipitate was filtered and re-suspended in a mixture of 150mL of de-ionized water and 150mL of acetone and let stir for 15 minutes. The product was filtered and re-suspended in another solution of hot methanol, then allowed to cool slightly and 50mL of acetonitrile and de-ionized water were added. When the mixture reaches room temperature it was filtered again, resulting in 2.1g (75 % yield) of pure white powder after drying overnight in a dessicator. <sup>1</sup>H NMR (400MHz, CDCl<sub>3</sub>, 50°C) δ = 7.32 (m, 10H), 6.78 (m, 18H), 4.76 (s, 4H), 4.49 (s, 8H), 3.79 (s, 8H), 3.56 (s, 4H), 2.79 (s, 12H). <sup>13</sup>C NMR (400MHz, CDCl<sub>3</sub>, 50°C) δ = 127.4-130.3, 122.1-122.0, 75.6, 67.0, 32.5, 31.6, 31.5.

Preparation of **7** (37, 40-Diallyloxy-38, 39, 41, 42-tetra(1-methylimidazolyl)oxy-dihydroxycalix[6]arene)

In a 100ml round bottom flask, 40mL's of THF and 20mL's of DMF (9:1) were placed on a magnetic stirrer and set to mix. Then, 2.0g (0.0028mol) of **3B** were added to the round bottom and put in a 0°C ice bath for five minutes. Once the mixture has cooled it is removed from the ice bath. Next, 3.4g (0.084 mol) of NaH (as a 60% oil dispersion) was washed twice with hexane and added in small portions to the reaction mixture and allowed to stir for an additional fifteen minutes. Finally, 3.6 g (0.017 mol) of N-methyl-2-chloromethyl imidazole were added portion-wise to the reaction mixture and allowed to react for one hour at room temperature under argon. After an hour, the THF was removed under reduced pressure and the high vacuum was required to remove an amount of DMF to achieve a final volume that is approximately 1/3<sup>rd</sup> the original volume, and allowed to cool while stirring. To the stirring solution, 300mL of de-ionized water was added drop-wise. The resulting precipitate was filtered and re-suspended in a mixture of 150mL of de-ionized water and 150mL of acetone and let stir for 15 minutes. The product was filtered and re-suspended in another solution of hot methanol, then allowed to cool slightly and 50mL of acetonitrile

and de-ionized water were added. When the mixture reaches room temperature it was filtered again, resulting in 2.0g (75 % yield) of pure white powder after drying overnight in a dessicator.  $^1\text{H}$  NMR (400MHz,  $\text{CDCl}_3$ ,  $50^\circ\text{C}$ )  $\delta$  = 6.82, (m, 18H), 5.8 (s, 2H), 4.98 (d of d, 4H), 3.94, (s, 4H), 3.79 (s, 8H), 3.59 (s, 4H), 3.43 (s, 8H), 3.01 (s, 12H).  $^{13}\text{C}$  NMR (400MHz,  $\text{CDCl}_3$ ,  $50^\circ\text{C}$ )  $\delta$  = 134.1, 129.9-122.3, 118.0, 74.2, 66.9, 32.6, 31.7, 31.6.

#### UV-Vis experiments

For the mole ratio method, two solutions of equal molarity were made; one of 7 and one of  $\text{Cu(II)NO}_2$ . Both compounds were dissolved in an 80:20 solution of DCM:MeOH. The total volumes for all samples were kept constant at 200  $\mu\text{L}$ . The mole ratio was equated to the volume of each compound since they were equimolar solutions. For example, a mole ratio of 0 is equal to 200  $\mu\text{L}$  of  $\text{Cu(II)NO}_2$  and 0  $\mu\text{L}$  of calixarene. The next sample would be 190  $\mu\text{L}$  of  $\text{Cu(II)NO}_2$  with the remaining 10  $\mu\text{L}$  being calixarene, and so on until a mole ratio of 1 was achieved. The charge transfer band was observed at 694nm and plotted as a function of mole ratio of calixarene. Mole ratios of 0 and 1 were not included in the mole ratio plot, only as confirmation of no absorbance at 694nm.

In the Hill plot experiment, the amount of calixarene was kept constant throughout the entire set of data points. A solution of **7** was diluted in an 80:20 solution of DCM:MeOH and a 1mL aliquot was placed in a sample tube. Cu(II)NO<sub>2</sub> was added stepwise in 0.1eq's increments until 3eq's were reached. The absorbance at 694nm was recorded after each increment of copper was added and the absorbance was then plotted against equivalents of copper.

#### Mass Spectrometry Experiments

Typical conditions in the positive ion mode used for the electrospray ionization method on the LCQ mass spectrometer were a sheath gas flow rate of 40lpm, 200°C capillary temperature, +2kv capillary, +40kv tip, and a sample flow rate of 5-10µL/min. Compound **7** was diluted to 2.5x10<sup>-5</sup>M in 100% MeOH and sonicated into solution. Separate solutions for different stoichiometric ratios of copper and calixarene were made individually. Mass spectrometric data were collected over a period of one minute, and typically 12 spectra were averaged within that period. The mass spectrometer was tuned and calibrated daily before experiments were run. Results were validated by bracketing the samples with calibration standards.

## Gel Electrophoresis Experiments

Single stranded oligonucleotides (Ax50, Tx50, Gx50, Cx50) were ordered from Bioserve and annealed (poly AT, poly GC) by heating for 10-15minutes at 100°C, then cooled. Pre-cast, 20% polyacrylamide gels were purchased from Invitrogen along with a 10bp ladder. Each lane was loaded with 200ng of DNA and calixarene was loaded at 0.1 eq of DNA. Various amounts of copper were added to study the affects on hydrolysis. The DNA/ calixarene/ copper mixture was suspended in a 50:50 solution of DMSO and sterilized water, with 10mM Tris adjusted to pH 7.5. Samples were incubated at 37°C for three hours before adding running buffer and loading onto the pre-cast gels at 200v (15milliamps) for 2 hours, or until finished. Finally, the DNA was visualized with ethidium bromide staining and exposure under UV light.

## Molecular Modeling Experiments

Atom coordinates (abc) from the .CIF file for 7 were entered into the Acclerys Cerius<sup>2</sup> software via the crystal building module, and the solvent was left out. Protons were added with the Add H function on the 3D-Builder panel. Next the atomistic forcefield COMPASS, reported by Sun and Ren<sup>27</sup> and Sun<sup>28</sup>, was loaded to calculate the most probable positions of the protons. Next, the

molecule was assigned charges in the open forcefieldsetup module and minimized in open forcefield methods module<sup>29-48</sup>. The molecule, minus the protons, was restrained during this calculation using the constraints function in the minimizer module, and only the protons were minimized. Then the forcefield was switched to UNIVERSAL where all calculations were done with the copper binding studies. A single Cu<sup>2+</sup> atom was placed near one of the symmetrical ends of the molecule and minimized. After minimization, dynamics were run at 298 K and 0.1 GPa of pressure with 1000 steps of 0.001 ps per step. This two step processes of dynamics/minimization was done until the most stable 1:1 conformer was achieved. Another Cu<sup>2+</sup> atom was then added to the other end of the molecule, opposite of the first copper and steps of minimization/ dynamics were repeated again to achieve the most stable 2:1 complex.

## REFERENCES

- 1 Izquierdo, M. *Cancer Gene Therapy*. **2005**, 12, 217-227.
- 2 Elbashir, S.M.; Lendeckel S., Tuschli T. *Genes Rev.* **2001** 15,188-200.
- 3 Reinhoudt, D.N.; Molenveld, P.; Engbersen J.F.J.; et al. *J. Am. Chem. Soc.* **1998**, 120, 6726-6737.
- 4 Ghosh, M.; Meiss, G.; Pingoud, A.; London, R.E.; Pedersen, L. *J. Biol. Chem.* **2005**, 280, Issue 30, 27990-27997.
- 5 Reinaud, O.; Rondelez, Y.; Seneque, O.; et al. *Chem. Eur. J.* **2000**, 6,2418-4226.
- 6 Reinhoudt, D.N.; Molenveld, P.; Engbersen, J.F.J. *J. Org. Chem.* **1999**, 64, 6337-6341.
- 7 Inoue, Y.; Sakamoto, S.; Tamura, T.; et al. *Acids Res.* **2003**, 31, No. 5.
- 8 Terenzi, H.; Oliveira, M.C.B; Couto, M.S.R.; et al. *Polyhedron*. **2005**, 24, 495-499.
- 9 Reinaud, O.; Rondelez, Y.; Rager, M.; et al. *J. Am. Chem. Soc.* **2001**, 124, No. 7.
- 10 Reinaud, O.; Seneque, O. *Tetrahedron*. **2003**, 59, 5563-5568.
- 11 Reinhoudt, D.N.; Molenveld, P.M.; Engbersen, J.F.J. *Angew. Chem. Int. Ed.* **1999**, 38, 3189-3191.
- 12 Chakravarty, A.R.; Dhar, S.; Nethaji, M. *Inorg. Chimica Acta*. **2005**, 358, 2437-2444.

- 13 Nishihara, H.; Korupoju, S.R.; Mangayakaraski, N.; et al. *Inorg. Chem.* **2002**, *41*, 4099-4101.
- 14 (a) Ragunathan, K; Schneider, H. *Angew. Chem. Int. Ed. Engl.* **1996**, *35*, 7472 (b) Williams, N.; Chin, J. *J.Chem. Soc. Chem. Commun.* **1996**, 131.
- 15 Sissi, C.; Mancin, F.; Gatos, M.; Palumbo, M.; Tecilla, P.; Tonellato, U. *Inorg. Chem.* **2005**, *44*, 2310-2317.
- 16 Miller, M.D.; Cai, J.; Krause, K.L. *J. Mol. Biol.* **1999**, *288*, 975-987.
- 17 Shlyapnikov, S. V.; Lunin, V. V.; Perbandt, M.; Polyakov, K. M.; Lunin, V. Y.; Levdikov, V. M.; Betzel, C.; Mikhailov, A. M. *Acta Crystallogr. Sect. D Biol. Crystallogr.* **2000**, *56*, 567-572.
- 18 Jin, Y.; Cowan, A. *J. Am. Chem. Soc.* **2005**, *127*, 8408-8415.
- 19 Sakamoto, S.; Tamura, T.; Furukawa, I.; Komatsu, Y.; Ohtsuka, E.; Kitamura, M.; Inoue, H. *Nuc. Acids Res.* **2003**, *31*, 5, 1416-1425.
- 20 Harford, C.; Sarkar, B. *Acc. Chem. Res.* **1997**, *30*, 123-130.
- 21 Lau, S.; Kruck, T.; Sarkar, B. *J. Biol. Chem.* **1974**, *249*, 5878-5884.
- 22 Long, E. *Acc. Chem. Res.* **1999**, *32*, 827-836.
- 23 Gutsche, C.; Dhawan, B.; No, K.; Muthukrishnan, R. *J. Am. Chem. Soc.* **1981**, *103*, 3782.
- 24 Reinhoudt, D. et al. *J. Am. Chem. Soc.* **1994**, *116*, 5814.
- 25 Otsuka, H.; Araki, K.; Sakaki, T.; Nakashima, K.; Shinkai, S. *Tetrahedron Letters.* **1993**, *34*, 7275.
- 26 Kanamathareddy, S.; Gutsche, C. *J. Am.Chem. Soc.* **1994**, *59*, 3871.
- 27 Sun, H.; Ren, P.; Fried, J.R. *Comput. Theor. Polym. Sci.* **1998**, *8*, 229-46.

- 28 Sun H. *J. Phys. Chem.* **1998**, 102, 7338–64.
- 29 Liang, C.; Ewig, C.S.; Stouch, T.R.; Hagler, A.T. *J. Am. Chem. Soc.* **1993**, 115, 1537–45.
- 30 Kavassalis, T.A.; Sundarajan, P.R. *Macromolecules* **1993**, 26, 4144–50.
- 31 Mayo, S.L.; Olafson, B.D.; Goddard, W.A. *J. Phys. Chem.* **1990**, 94, 8897–909.
- 32 Castonguay, L.A.; Rappe, A.K. *J. Am. Chem. Soc.* **1992**, 114, 5832–42.
- 33 de Vos Burchart, E.; Verheij, V.A.; van Bekkum, H.; van de Graff, B. *Zeolites* **1992**, 12, 183–9.
- 34 Garofalini, S.H.; Zirl, D.M. *J. Am. Ceram. Soc.* **1990**, 73(10), 2848–56.
- 35 Rappe, A.K.; Casewit, C.J.; Colwell, K.S.; Goddard, W.A.; Skiff, W.M. *J. Am. Chem. Soc.* **1992**, 114, 10024–35.
- 36 Maple, J.R.; Hwang, M-J.; Stockfisch, T.P.; Dinur, U.; Waldman, M.; Ewig, C.S.; et al. *J. Compos. Chem.* **1994**, 15, 162–82.
- 37 Hagler, A.T.; Huler, E.; Lifson, S. *J. Am. Chem. Soc.* **1974**, 96, 5319–27.
- 38 Sun, H.; Mumby, S.J.; Maple, J.R.; Hagler, A.T. *J. Am. Chem. Soc.* **1994**, 116, 2978–84.
- 39 Sun, H.; Ren, P.; Fried, J. *Comput. Theor. Polym. Sci.* **1998**, 8, 229–246.
- 40 Karasawa, N.; Goddard, W.A. *Macromolecules* **1992**, 25(26), 7268–88.
- 41 van Beest, B.W.H.; Kramer, G.J.; van Santen, R.A. *Phys. Rev. Lett.* **1990**, 64, 1955–8.
- 42 Lifson, S.; Hagler, A.T.; Dauber, P. *J. Am. Chem. Soc.* **1979**, 101, 5111–41.

- 43 Momany, F.A.; Carruthers, L.M.; McGuire, R.F.; Scheraga, H.A. *J.Phys.Chem.* **1974**, 78(16), 1595–620.
- 44 Nemethy, G.; Pottle, M.S.; Scheraga, H.A. *J. Phys. Chem.* **1983**, 87(11), 1883–7.
- 45 Williams, D.E. *J. Phys. Chem.* **1966**, 45, 3370–8.
- 46 Yashonath, S.; Thomas, H.; Nowak, A.K.; Cheetham, A.K. *Nature* **1988**, 331, 601–4.
- 47 Karawasa, N.; Goddard, W.A. *J. Phys. Chem.* **1989**, 93, 7320–7.
- 48 Allen, M.P.; Tildesley, D.J. *Computer simulation of liquids*. Oxford: Clarendon Press, **1987** p. 28.

## **APPENDIX: Additional Data and Spectra**

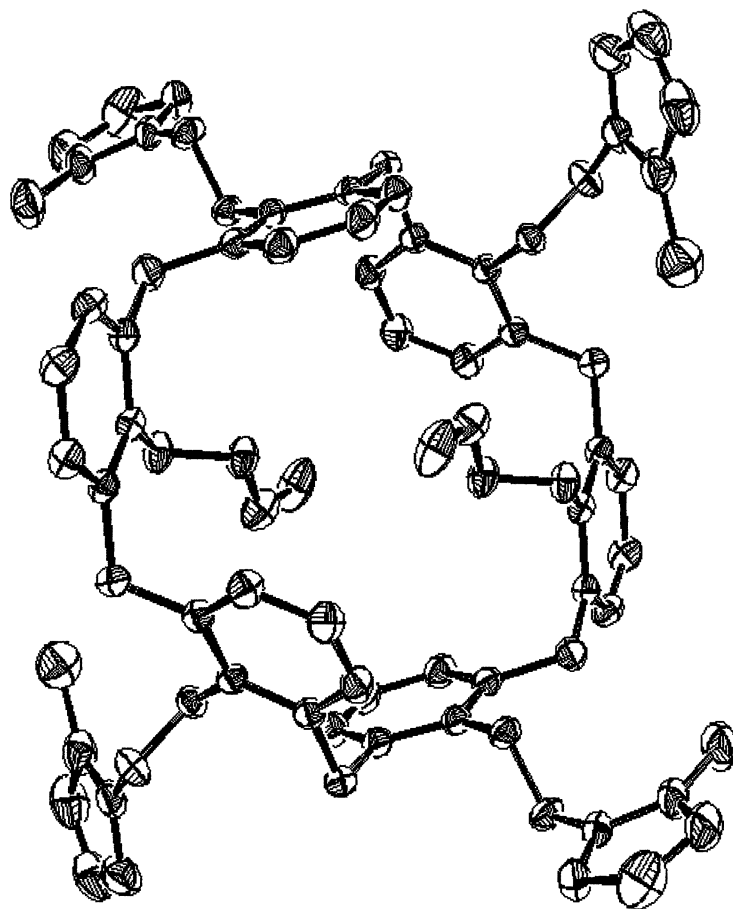


**Illustration 1** Crystal Structure of **7**.

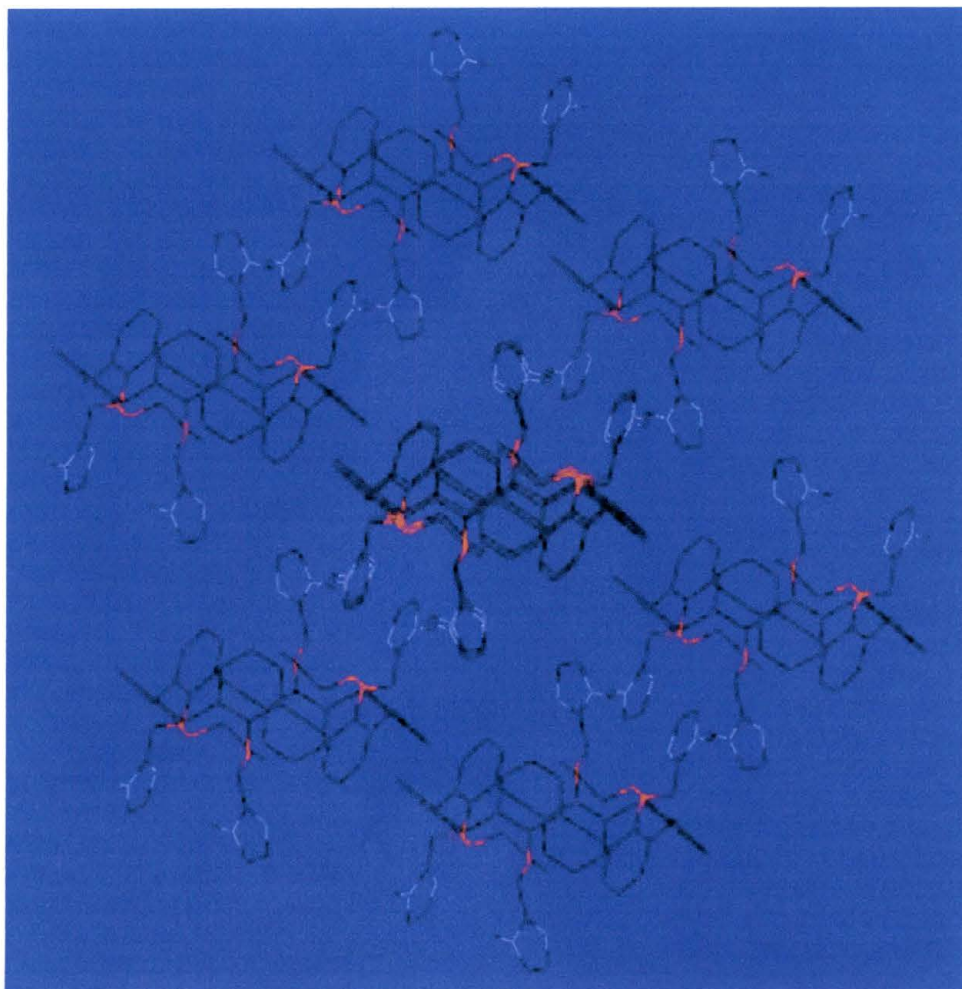
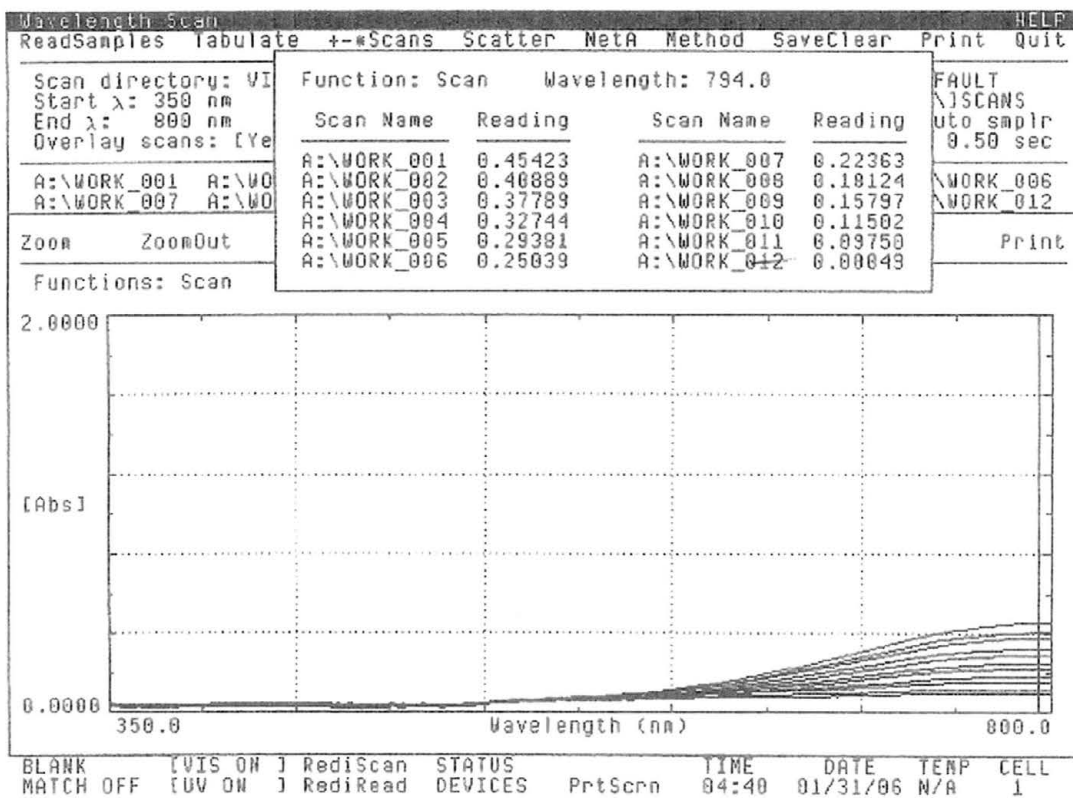
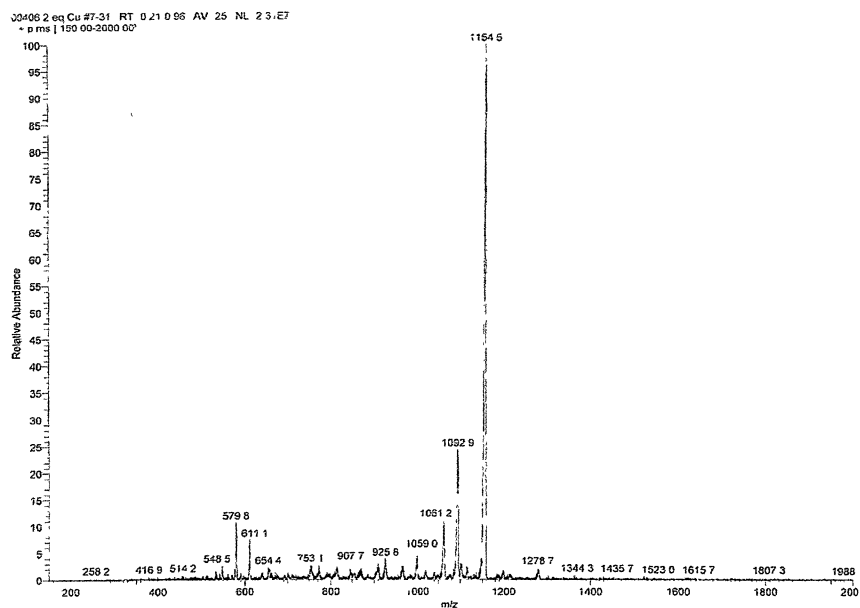


**Illustration 2** Unit Cell of 7.

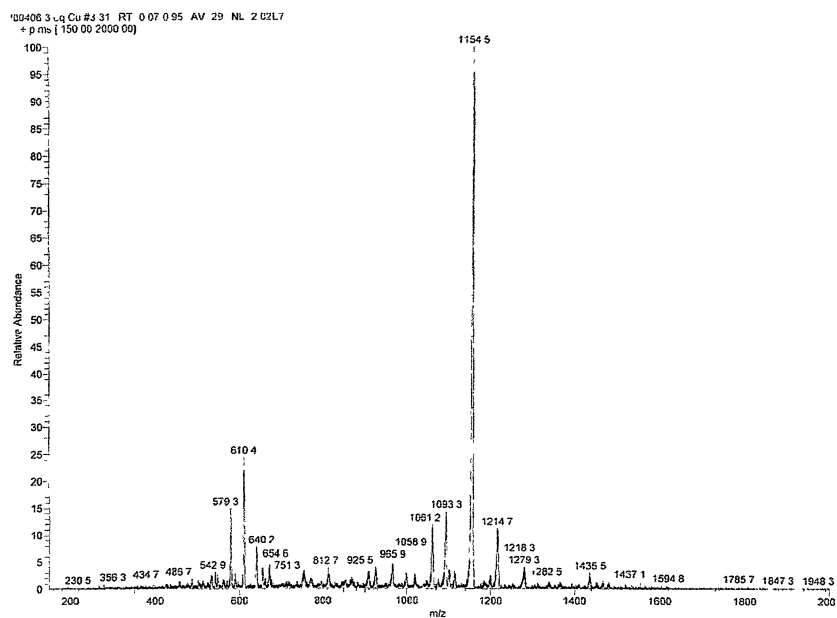




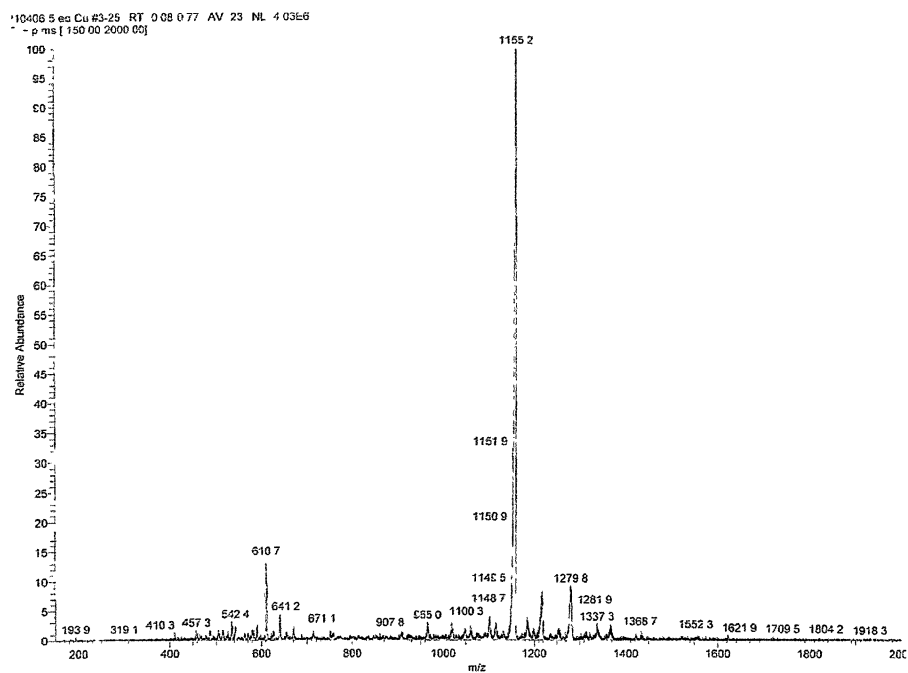
Spectra 2 UV-vis spectrum of copper only.



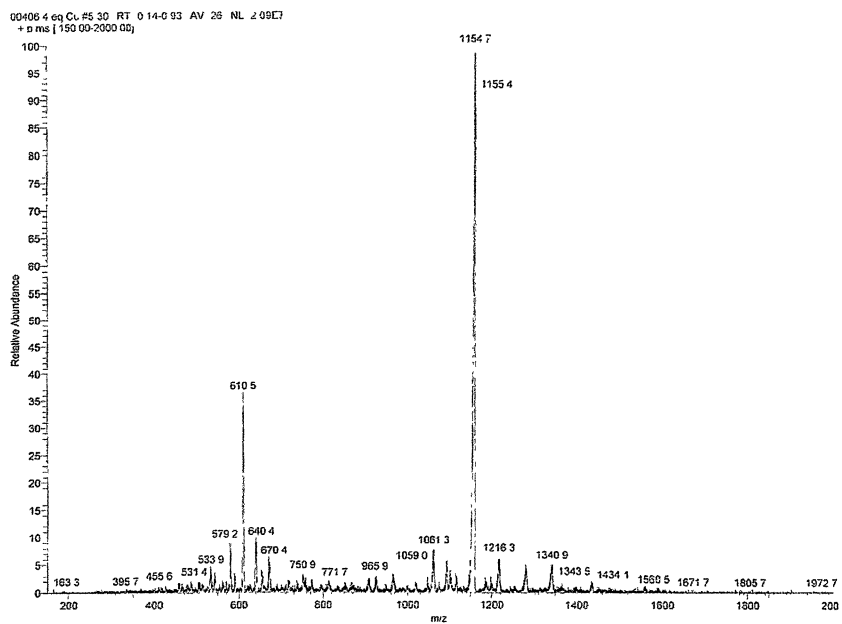
Spectra 3 ESI-MS data for two equivalents of copper.



Spectra 4 ESI-MS data three equivalents of copper.



**Spectra 5** ESI-MS data for four equivalents of copper.



**Spectra 6** ESI-MS data for five equivalents of copper.

## VITA

Derric Michael Borthwick was born in McLeod, Minnesota on October 21, 1981, the son of Kristi Daniels and Joseph Hacker. After graduating with honors from Romeoville High School, Romeoville, Illinois, in 2000, he accepted a full ride scholarship from the United States Marine Corps to attend the Virginia Military Institute and study chemistry. In May 2004, he was awarded the degree of Bachelor of Science in chemistry from VMI. Derric briefly worked as an analytical chemist before entering the graduate biochemistry program at Texas State University-San Marcos in January 2005. In anticipation of an August 2006 graduation, Derric accepted a position as a Sr. Chemist at a pharmaceutical company in Round Rock, Texas, May 2006.

Permanent Address: 2204 Wheaton Trail

Cedar Park, Texas 78613

This thesis was typed by Derric Michael Borthwick.